International Geotechnical Symposium on Theory and Practice of Earth Reinforcement / Fukuoka Japan / 5-7 October 1988
 ISBN 906191 820 0

Fabric reinforced retaining walls

Bengt B.Broms
Nanyang Technological Institute, Singapore

ABSTRACT: The design of fabric reinforced retaining walls is reviewed in the article. Methods are presented to calculate the lateral earth pressure acting on vertical and sloping walls and the evaluation of the force, spacing and length of the fabric reinforcement. The stability of the wall when the length of the fabric either increases or decreases with increasing depth also has been investigated.

1 INTRODUCTION

Investigations of the possible applications of woven high strength synthetic fabrics as reinforcement in soil first started about 25 years ago in order to increase the bearing capacity of embankments and footings or to reduce the lateral earth pressure acting on sheet pile and retaining walls. In Fig 1 is shown a fabric reinforced retaining wall and an embankment constructed of L-shaped concrete elements. The fabric reinforcement has in this application a dual function in that it both reduces the forces initiating failure and increases the stability of the wall. The main purpose of the L-shaped face elements is protect the fabric against vandalism and direct sunlight. They can be made very light since the lateral earth pressure acting on the wall is very low as indicated in the paper. It is also possible to shotcrete the face.

Several synthetic polymers are used as reinforcement in soil such as polypropylene, polyester, polyethylene, polyamide and glass fibres. A wide variety of both woven and non-woven fabrics are available where the fibres

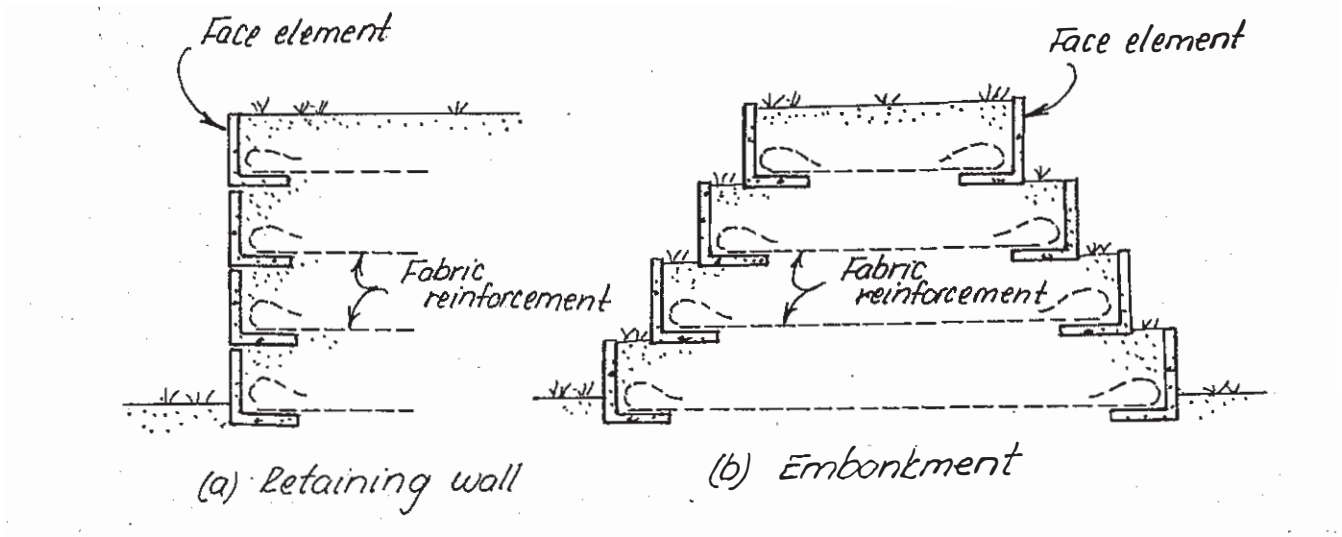

Fig.1 Applications of fabric as reinforcement in soil

are either bonded or interlocked. Also composite materials are used with a high resistance to environmental attacks.

Geofabric has several advantages as reinforcement in soil compared with steel or aluminium strips since the fabric has a high tensile strength and is flexible and thus not affected by large settlements. There are materials available with a tensile strength of up to 400 kN/m or more. Also the durability is high when the fabric is not exposed to direct sunlight. The surface area of the geofabric is large so that the force in the fabric can be transferred effectively to the soil. The required anchor length is thus short. The application of fabric as reinforcement in soil is, therefore, often a very economical method compared with other soil improvement methods since heavy equipment or skilled labour are not required for the construction. The reduction of the cost has in some cases been substantial, 40% or more compared with alternate methods.

The main disadvantages and limitations with geofabric when used as reinforcement in soil are the large deformations required to mobilize the tensile strength of the fabric, the lack of experience with the method especially about the long term performance as discussed in the paper and that the fabric had to be protected against direct sunlight which is particularly important for polypropylene. The deformations can be reduced by prestretching. There are also some questions about the durability (van Zanten, 1986) and that the fabric can be damaged when crushed rock or gravel is used as backfill. The sharp corners of the rock may puncture the fabric locally thereby reducing the tensile strength. The rupture strain can also be reduced but the stiffness is practically unchanged. It is therefore important that the fabric is protected against mechanical damage and chemical attacks. The material is also difficult to splice. The tensile strength of the seams can be only 50% of that of the unspliced material.

In this paper, the applications of geofabric as reinforcement in the backfill behind retaining walls and in embankments in order to reduce the lateral earth pressure and to increase the stability are reviewed. Design methods are proposed for retaining structures and high embankments reinforced with fabric based on the strength and deformation properties of the reinforcing material and on the interface friction and adhesion between the fabric and the soil.

2 STRENGTH AND DEFORMATION PROPERTIES OF GEOFARBIC

2.1 Stress-strain Relationship

Test methods have been developed to determine the strength and the stress-strain properties of geofabric used as reinforcement in soil. The factors which are of particular interest are :

* the short and long term tensile strength of the fabric when confined in the soil.
* the axial strain at working load and at failure and how it is affected by time (creep).
* the interface friction and adhesion between fabric and soil

The main uncertainties are the effect of time and the environment on the ultimate strength of the geofabric and on the bearing capacity of the soil and the increase with time of the lateral displacements and of the settlements caused by creep. Colin et al (1986) have investigated the tensile strength of fabric that has been buried in soil.

Uniaxial and biaxial tensile tests are commonly used to determine the short and long term tensile strength and the deformation properties of both woven and non-woven fabric materials (e.g. Myles, 1986). There are a number of short-comings with some of these testing methods. At, for example, strip load tests it is difficult to load the sample uniformly since the strain distribution is not uniform across the sample during the loading. Necking occurs at the centre when the ultimate strength is approached.

Accelerated creep tests (elevated temperature) are used to determine the creep rate and the long term tensile strength. However, the results from creep tests should not be extrapolated over more than two log-cycles of time as pointed out by Jewell and Greenwood (1988).

It is also well known that the confinement of the fabric in the soil improves its mechanical properties. For example, the axial strain in the fabric

will be reduced considerably with increasing confining pressure. Confined tensile tests have been carried out by McGown et al (1981), El-Fermoui and Nowatzki (1982) Andrawes et al (1984) and by Chandrasekaran (1988).

A specially designed box (63.5 x 63.5 mm) was used by El-Fermoui and Nowatzki (1982) so that a normal pressure could be applied to the fabric during the testing. At the tests carried out by McGown et al (1981) and Andrawes et al (1984) a normal pressure was applied by means of rubber bellows on both sides of the fabric which was embedded in soil. The test results indicated that the stiffness and the tensile strength of the non-woven fabric increased with increasing confining pressure. The tensile strength of the woven fabric when confined was approximately the same as that of the unconfined samples. The confinement reduced somewhat the strain at failure while the stiffness of the fabric was increased. The main effect of the confinement was to reduce the lateral contraction of the fabric sample during the testing so that the stress distributed across the sample became much more uniform.

Both unconfined and confined direct tension tests have been carried out by Chandrasekaran (1988). Test results indicated that the tensile strength of the woven fabric was somewhat less than that of the single threads (yarn). Part of this difference could be attributed to the non-uniform strain distribution across the fabric samples during the testing. The confined tension tests were carried out inside a 300 mm diameter steel cylinder lined on the inside by a rubber membrane so that a confining pressure could be applied to the sand and thus to the fabric embedded in the sand. The strain distribution along the fabric was measured with strain gauges which were glued to the fabric. In Fig 2 is shown the stress-strain properties of the investigated woven polyester fabric at different confining pressures (100, 150, 200 and 300 kPa). It can be seen that the axial deformation of the fabric was reduced when the confining pressure was increased. At 30% to 50% of the ultimate strength of the fabric material, the working load, the axial strain was only 40% to 60% of the axial strain of the unconfined samples when the confining pressure was 300 kPa. The test data indicated that the ultimate strength of the fabric was not affected by the confining pressure.

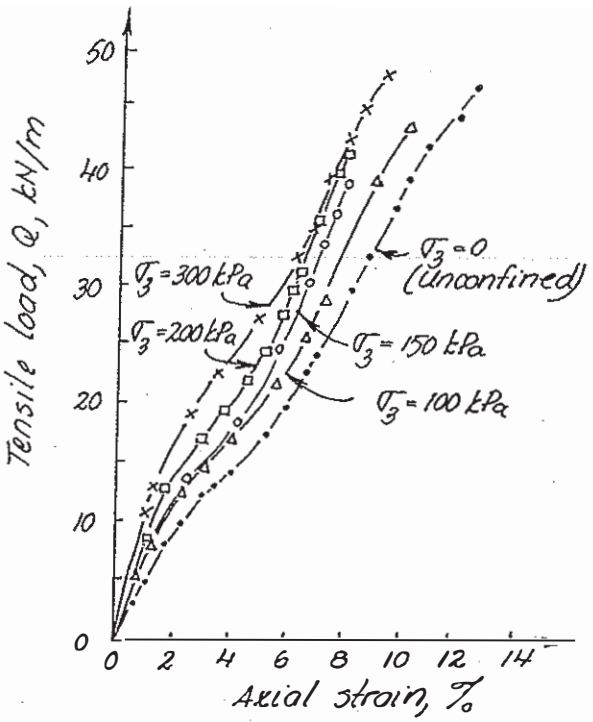

Fig.2 Tensile load versus axial strain curve for woven polyeter fabric at different confining pressures (after Chandrasekaran, 1988)

Christopher et al (1986) investigated the effect of confinement with zero span tension tests where the distance between the two clamps is small. The test results from the zero span tension tests are very uncertain since the strain distribution is not uniform between the clamps. Slippage of the clamps affects the results as well.

2.2 Interface Friction Angle (ϕ_a')

The soil-fabric interface friction angle (ϕ_a') has been evaluated by several (e.g. Holtz, 1977; Myles, 1982; Miyamori et al, 1986; Chandrasekaran, 1988)

(1) by pull-out tests and

(2) by direct shear box tests.

A special 1.10 x 0.25 m direct shear box was designed by Holtz (1977) so that 0.15 m wide fabric strips could be tested. The normal pressure was applied with a pressure bag and the stress distribution along the fabric strip was determined with magnets glued to the

fabric. The test data indicated that the interface friction angle (ϕ_a') of the investigated sand was the same as the angle of internal friction as determined by direct shear tests.

Myles (1982) used direct shear tests (100 x 100 mm) to investigate the soil-fabric interface friction. The fabric was located in the lower frame of the direct shear apparatus while sand was placed in the upper frame. The investigation indicated that the interface friction angle varied with the type of fabric material, woven and non-woven.

Miyamori et al (1986) investigated also the soil-fabric interface friction of non-woven fabric with direct shear tests. A relatively large shear box was used (316 x 316 mm). The interface friction resistance (ϕ_a') was found to be lower than the angle of internal friction of the investigated soil as determined by triaxial or direct shear tests. For dense sand the interface friction resistance was only 72% to 87% of the peak shear strength of the sand. A relatively large relative displacement was required to mobilize the peak resistance along the fabric because of the large thickness of the investigated non-woven material.

Direct shear tests were also carried out by Chandrasekaran (1988) to determine the soil-fabric interface friction. The size of the direct shear box was 100 x 100 mm. It was found that the interface friction angle of the investigated angular sand decreased with increasing normal pressure from about 41° at a low normal pressure (50 kPa) to about 32° when the normal pressure was 500 kPa as shown in Fig 3. The angle of internal friction of the sand as determined by drained triaxial tests was 39°. The reduction of the interface friction angle with increasing confining pressure was thus substantial. The interface friction angle has also been found to be affected by size of the openings in the fabric. The openings of the investigated woven polyester fabric were about 0.1 mm while the average particle size of the sand was 1.2 mm. The corresponding interface friction angle was 34.3°. For cotton gauze where the size of the openings was about 1.0 mm, the average interface friction angle was about 40° which is approximately equal to the angle of internal friction as determined by triaxial tests (39°).

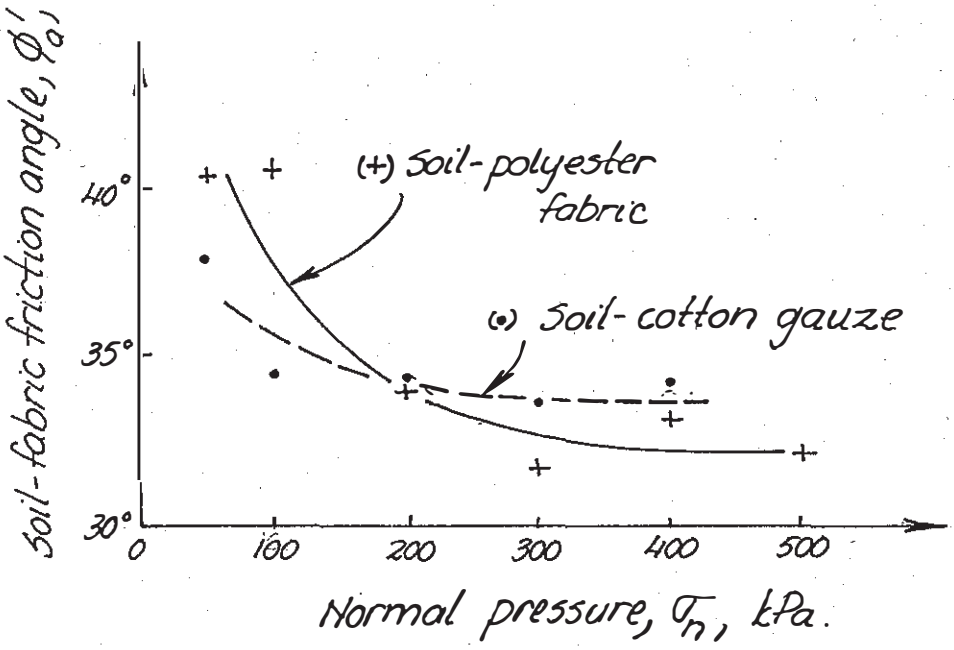

Fig.3 Variation of interface friction angle with normal pressure; woven polyester fabric and cotton gauze

3 FABRIC REINFORCED SOIL

The behaviour of the fabric reinforced soil can be demonstrated by triaxial tests as illustrated in Fig 4 where the fabric reinforcement is placed in horizontal layers in the soil as discussed by Broms (1977). This test method was first used by Schlosser and Long (1974) to investigate the effect of aluminium foil on the strength and deformation properties of sand. The spacing of the horizontal aluminium disks and the relative density of the sand were varied. The test results show that both the strength and deformation properties of the sand were improved noticeably. Two different failure modes were observed. At a low confining pressure, failure occurred by slippage along the reinforcement when the interface friction was fully mobilized (Fig 5). In this case the ultimate strength is governed by the interface friction angle. The shear strength of the reinforced soil was characterized by an apparent friction angle which is larger than the effective angle of internal friction of the soil (ϕ'). At

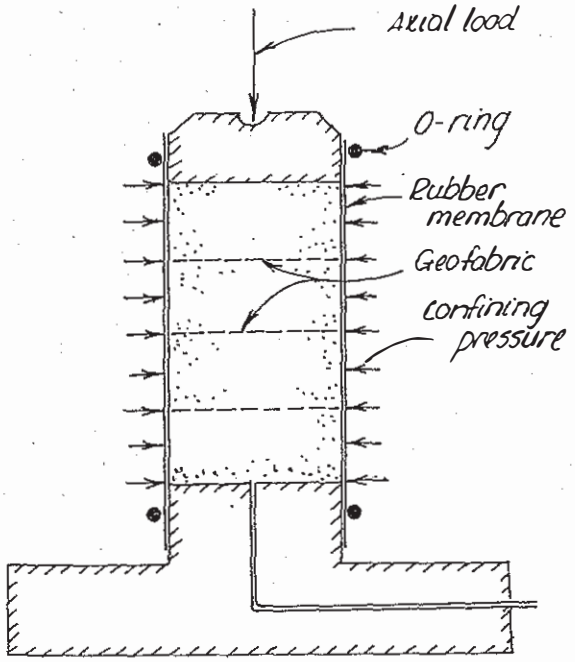

Fig.4 Triaxial tests with fabric reinforcement

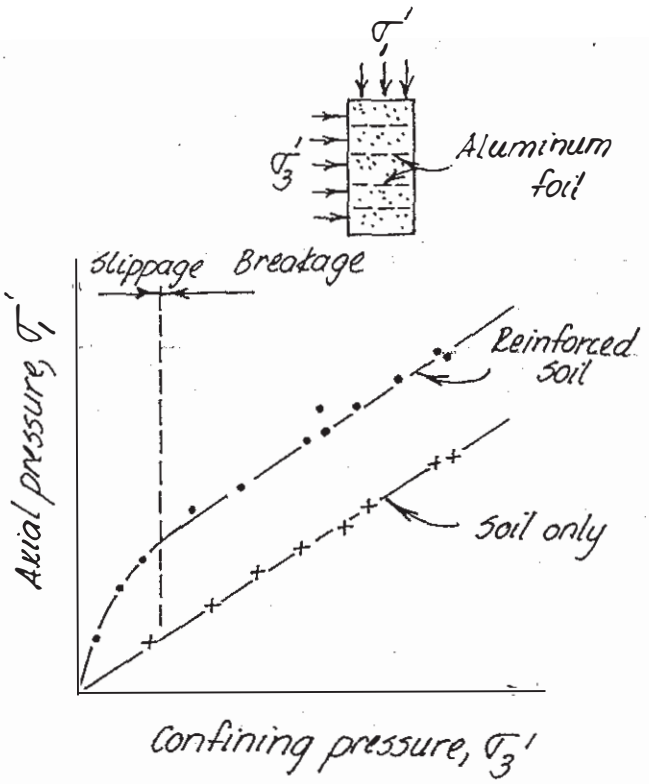

Fig.5 Failure curves for triaxial reinforced and unreinforced sand samples (after Schlosser and Long, 1974)

a high confining pressure, the ultimate strength of the samples is governed by the tensile strength of the disks. In this case, the ultimate strength of the reinforced soil is characterized by an apparent effective cohesion (c_r)

$$c_r = \frac{T}{D}\sqrt{K_p} \qquad (1)$$

where T is the tensile strength of the reinforcement (kN/m), D is the vertical spacing of the reinforcement and K_p is the coefficient of passive earth pressure. The friction angle corresponds to the effective angle of internal friction (ϕ') as illustrated in Fig 5.

Long et al (1983) investigated the stress distribution in triaxial samples reinforced with horizontal bronze discs. They found that the stress distribution along the discs was not uniform. The maximum interface friction resistance was mobilized near the edge of the disks. At the periphery of the sample the shear stress was significantly lower than the peak resistance. At the centre the resistance was zero since the

relative displacement between the reinforcement and the soil was zero due to symmetry.

Broms (1977) investigated the stress-strain properties of triaxial samples reinforced with fabric disks. At these tests, the relative density of the sand and the spacing of the fabric layers were varied. The experiments indicated that the compressive strength of the cylindrical samples increased with decreasing spacing of the reinforcement and with increasing confining pressure. It was shown that the restraint offered by the reinforcement was equivalent to that of a confining pressure. The coefficient of lateral earth pressure K_b next to the fabric was estimated from the relationship

$$K_b = \frac{1}{1 + 2 \tan^2 \phi'_a} \qquad (2)$$

where ϕ'_a is the effective interface friction angle.

Halfway between two fabric layers the coefficient of active earth pressure K_a will govern since the shear stress along a horizontal plane through the sample is equal to zero due to symmetry.

$$K_a = \frac{1 - \sin \phi'}{1 + \sin \phi'} \qquad (3)$$

It was proposed to use an average value K_{av} on the coefficient of lateral earth pressure in the calculations of the equivalent confining pressure.

$$K_{av} = 1/2 \, (K_a + K_b) \qquad (4)$$

The vertical stress distribution along the fabric is then given by the equation

$$\sigma'_v = \sigma'_{vo} \, e^{\frac{2 \tan \phi'_a}{DK_{av}}(r_o - r)} \qquad (5)$$

where σ'_{vo} is the vertical stress at the perimeter of the sample ($r = r_o$), ϕ'_a is the effective interface friction angle, r is the distance from the centre of the sample and D is the spacing of the fabric layers. Eq (5) thus indicates that the vertical normal stress increases rapidly towards the centre of the sample.

It has thus been assumed in the derivation of this equation that the total tension force in the fabric at the periphery of the sample is equivalent to a uniformly distributed confining pressure and that the shear strength is fully mobilized along the soil-fabric interface. This is not the case at the centre of the sample where the relative displacement of the soil with respect to the fabric reinforcement is equal to zero. The increase of the bearing capacity depends mainly on the friction resistance along the reinforcement and thus on the interface friction angle ϕ'_a. This friction angle is also affected by the stiffness of the reinforcement. It is lower for a non-woven than for a woven fabric.

The stress distribution in triaxial samples reinforced with aluminium foil, aluminium mesh and non-woven bonded fabric has been investigated by McGown et al (1978). They classified the reinforcement in the soil as inextensible and extensible depending on the failure mode of the samples. The reinforcement was classified as relatively inextensible when the reinforcement failed before the soil. In this case, the behaviour of the soil is brittle and the failure occurs suddenly without much warning. The term relatively extensible reinforcement was used when the sample failed before the reinforcement. The failure of the soil occurs in this case gradually. The behaviour is ductile and the reduction of the capacity beyond the peak strength is small.

Chandrasekaran (1988) has also investigated the behaviour of fabric reinforced soil using triaxial tests. The 100 mm or 200 mm diameter samples with angular medium coarse sand which were investigated were reinforced with horizontal fabric disks. Both woven and non-woven fabrics were tested. The spacing of the disks and the relative density of the sand were varied. The strain distribution along the fabric was measured with strain gauges attached to the fabric at different locations.

Typical stress-strain curves for the 100 mm diameter samples reinforced with woven polyester fabric disks are shown in Fig 6 at an applied confining pressure of 50 kPa. It can be seen that the ultimate strength increased with increasing number of layers and that the maximum increase was over 200% when

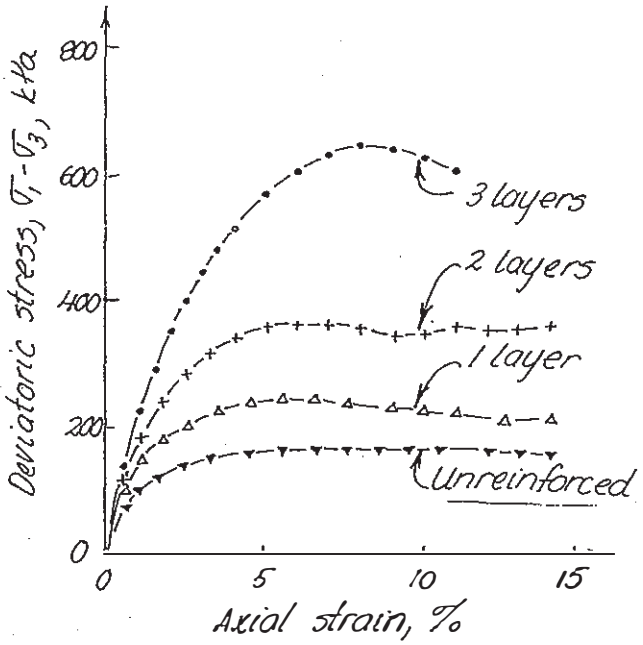

Fig.6 Stress-strain curves obtained for unreinforced and polyester fabric reinforced samples; confining pressure = 50 kPa (after Chandrasekaran, 1988)

three layers were used. Failure occurred by slippage along the fabric. It was found that stiffness of the sample was increased by the fabric as well as the deformation required to mobilize the peak strength.

The relative increase of the strength with decreasing spacing of the fabric layers has been plotted in Fig 7 at different confining pressures. It can be seen that the relative increase of the bearing capacity increased with increasing confining pressure.

The stress-strain relationships for the 200 mm diameter samples reinforced with woven polyester fabric disks are shown in Fig 8. The spacing of the layers was varied. The peak strength of the samples with three layers of reinforcement was governed by the tensile strength of the fabric as can be seen by the rapid drop of the capacity when the axial strain exceeded 12%. The ultimate strength of the sample reinforced by a single layer was governed by the interface friction angle (ϕ_a') rather than by the tensile strength of the fabric. The decrease of the resistance beyond the peak resistance was small.

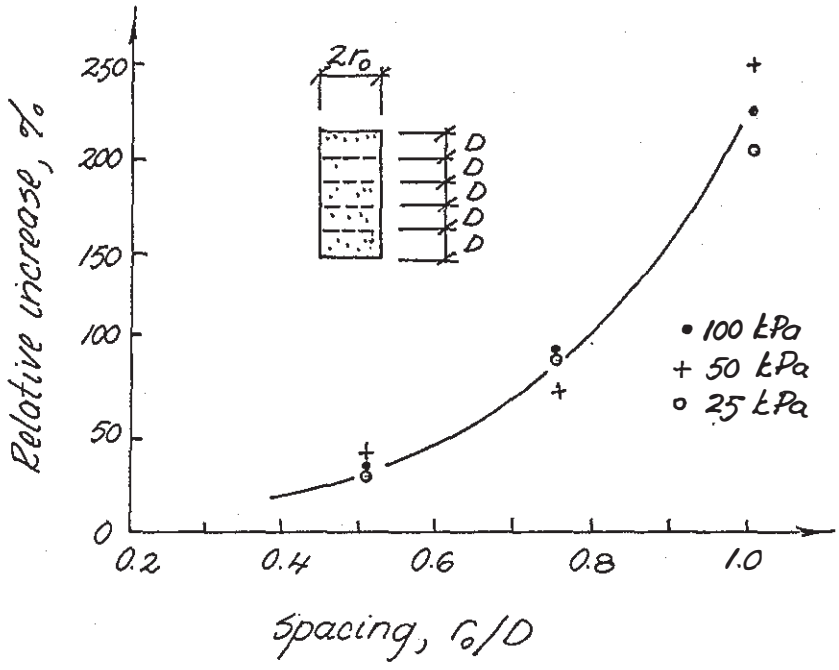

Fig.7 Relative increase in peak axial load of reinforced samples with decrease in fabric spacing

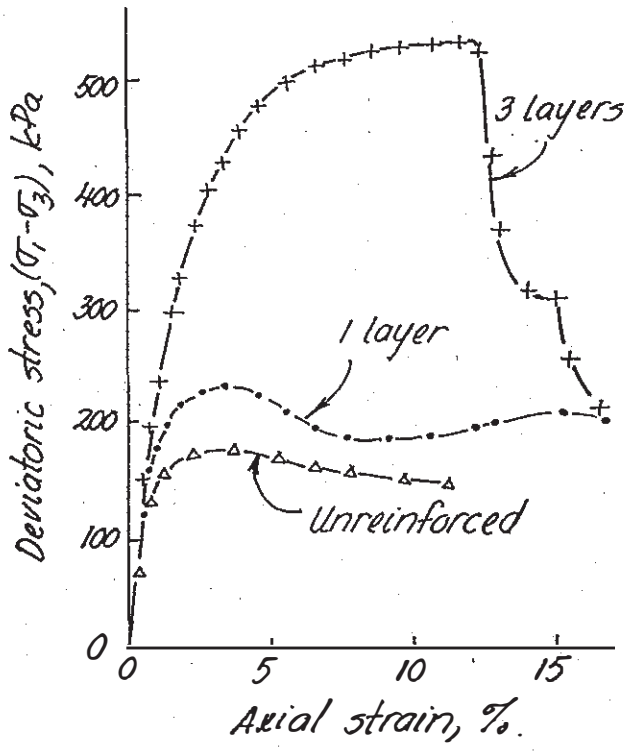

Fig.8 Stress-strain relationship for 200 mm diameter triaxial samples; confining pressure = 50 kPa

The strain distribution along the fabric reinforcement has been plotted in Fig 9. It can be seen that the axial strain in the fabric increased towards the centre of the sample. The gradient corresponds to the shear stress distribution along the fabric. The maximum shear stress and the maximum gradient were observed along the perimeter of the sample since the relative displacement there between the fabric and the soil was large. At the centre the shear stress is equal to zero because of the small relative displacement between the fabric and the soil.

The non-uniform shear stress distribution can be taken into account by assuming that the mobilized friction resistance along the fabric increases linearly from the centre of the sample toward the periphery and that the maximum mobilized interface friction angle is ($\alpha\phi_a'$) at the periphery of the sample. It has been observed that the mobilized friction angle ($\alpha\phi_a'$) for woven fabrics was less than the interface friction angle (ϕ_a') as determined by e.g. direct shear tests. This reduction can be expressed by the coefficient α. Thus

$$\tau_a = \sigma_v' \frac{r}{r_o} \tan \alpha\phi_a' \qquad (6)$$

where r is the radical distance from the centre of the sample, r_o is the radius, ϕ_a' is the interface friction angle and α is a reduction factor which can be as low as 0.5 for non-woven fabrics. For woven fabrics test data indicate that $\alpha = 1.0$.

The vertical stress distribution along the fabric can then be estimated from the equation

$$\sigma_v' = \sigma_{vo}' \, e^{\left[\frac{\tan \alpha\phi_a' \, (r_o^2 - r^2)}{DK_{av} \quad r_o}\right]} \qquad (7)$$

where σ_{vo}' is the vertical effective stress at the perimeter of the sample ($\sigma_{vo}' = \sigma_{ho}' K_a$). D is the spacing of the fabric layers and $K_{av} = 1/2 (K_a + K_b)$.

A comparison between calculated and measured ultimate (peak) strengths as

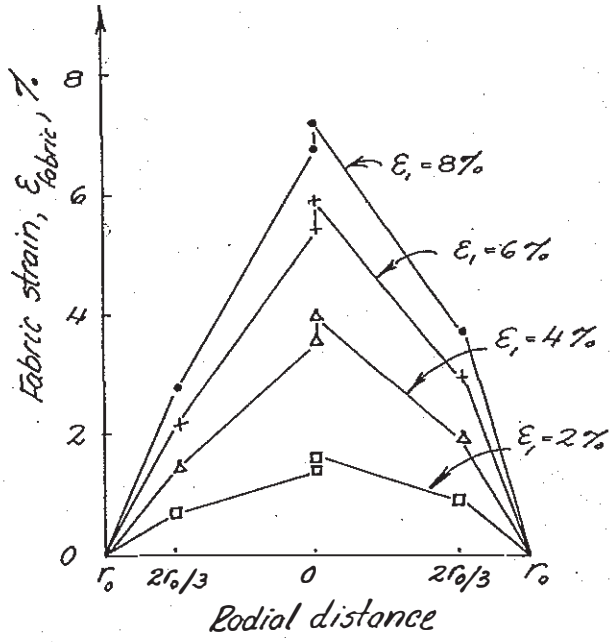

Fig.9 Typical plot of fabric strain gradient along the radius of the fabric disc; triple layered sample

evaluated from Eq (7) is shown in Figs 10a and 10b for samples with 100 mm and 200 mm diameter, respectively. The agreement with the modified calculation method has improved considerably compared with the original model (Eq. 5). The test results data thus indicate the importance of the relative displacement of the fabric with respect to the soil and of the mobilized interface friction angle. The results show that the relative displacement had to be considered in the design of fabric reinforced retaining walls.

An attempt has also been made to analyze the stress distribution in the fabric reinforced samples, using the finite element method (FEM) and assuming an hyperbolic stress-strain relationship for the soil. One major limitation of

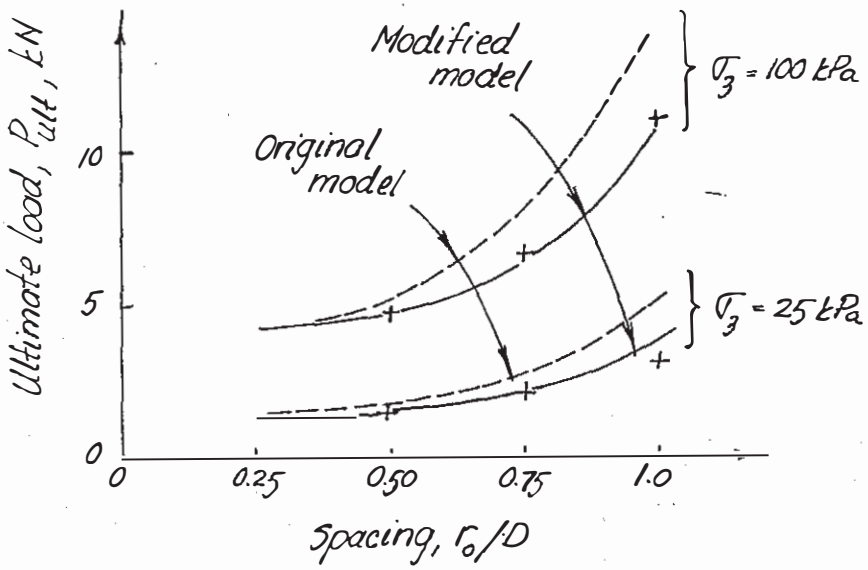

Fig.10a Comparison between experimental and computed peak axial loads; 100 mm diameter samples

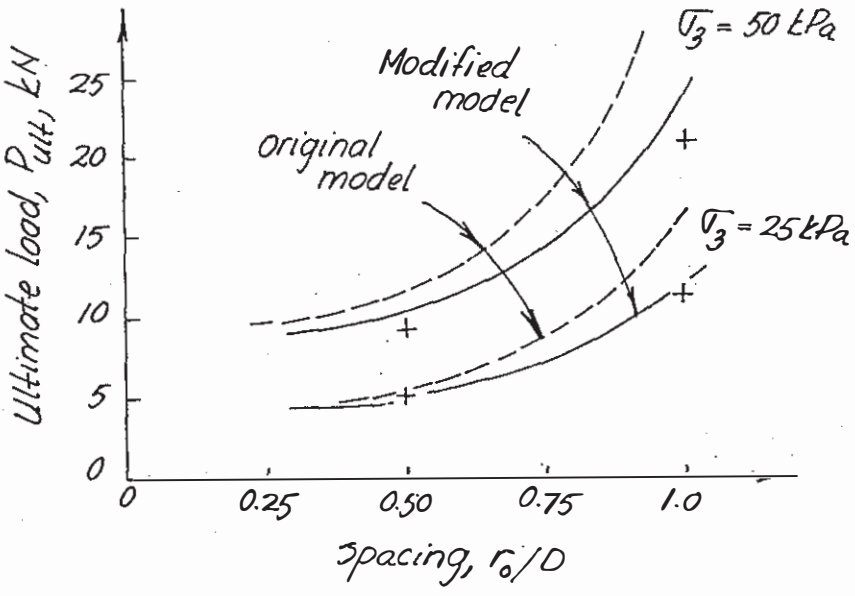

Fig.10b Comparison between experimental and computed peak axial loads; 200 mm diameter samples

the method is that the dilatancy of the soil cannot be considered. The calculated peak strength of the fabric reinforced samples by FEM was too high as well as the calculated stiffness of the soil.

The mobilized interface friction angle ($\alpha\phi_a'$) and thus the coefficient α were found to be affected by the fabric type, woven or non-woven. A much lower value (0.45 to 0.55) on the coefficient α was observed for the non-woven fabric due to the low stiffness compared with the investigated woven material. Also the spacing (D) of the layers affected the mobilized interface friction angle as well as the confining pressure.

Two different modes of failure was observed depending on the size of the samples, the confining pressure and the tensile strength of the fabric. Compression failure by slippage of the soil along the fabric occurred when the confining pressure was low and the spacing of the fabric layers was large. It was found that the axial strain increased gradually with increasing applied load. Tensile failure caused by tearing of the reinforcement occurred at the centre of the sample at a high confining pressure and a close spacing of the fabric layers. This type of failure occurred rapidly without previous warning. The capacity of the samples decreased suddenly when the sample was deformed further.

4 FABRIC REINFORCED RETAINING WALLS

4.1 Design Principles

Fabric can be used as reinforcement in the backfill behind retaining walls to increase the stability and to reduce the lateral earth pressure acting on the wall as discussed by e.g. Hausman (1976), Broms (1977), Ingold (1982) and Jones (1985). The spacing of the fabric layers is primarily governed by the long-term strength of the fabric, the interface friction or adhesion and by the total lateral earth pressure acting on the retaining structure. In the design of a fabric reinforced wall it is important to consider the variability of the strength of the fabric, the variability of the applied load, the consequences in case of a failure and the costs for the repair or reconstruction of the damaged wall. This can be done by using partial factors of safety.

The L-shaped elements shown in Fig 11

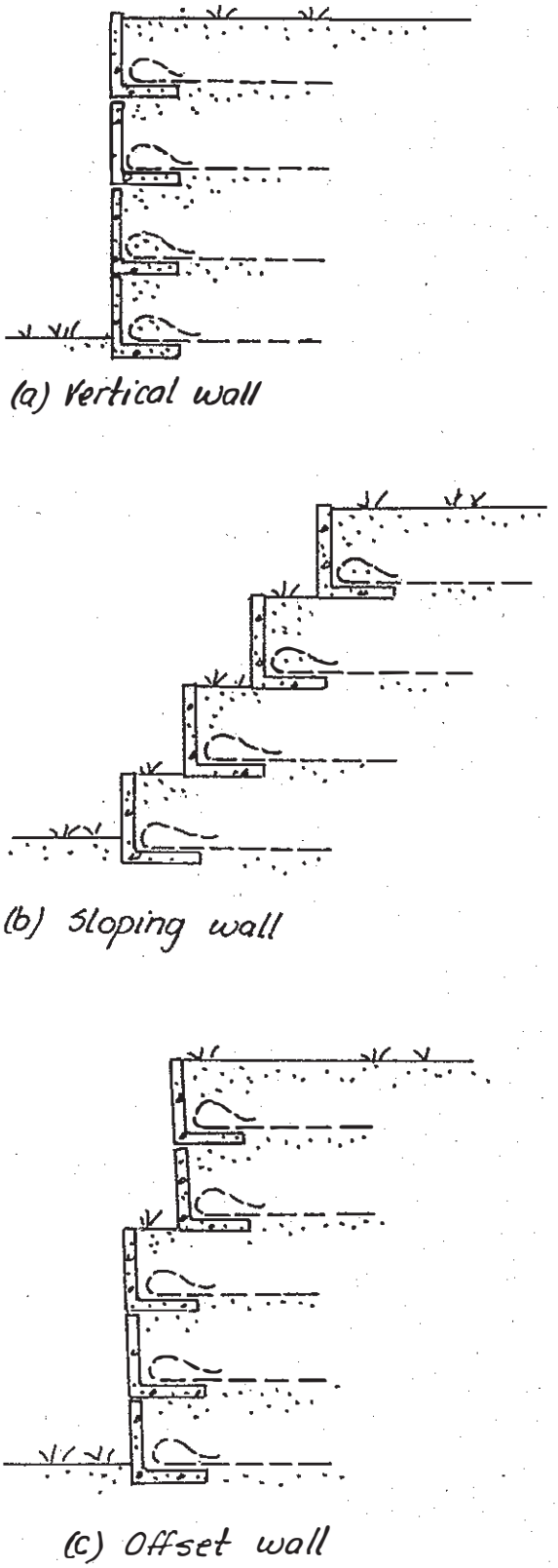

Fig.11 Applications of geofabric as reinforcement for retaining walls and slopes

can either be placed just above one another (Fig 11a) or be staggered (Fig 11b). Another possibility is shown in Fig 11c where two or three elements are grouped together. The L-shaped wall elements can be made relatively light as discussed in the following. The main function of the elements is to protect the fabric against vandalism and direct sunlight. It is also possible to fold the fabric and to protect the surface with shotcrete reinforced with wire mesh.

Granular soil (sand, gravel or rock fill) is usually used as backfill material because of the high interface friction angle which corresponds approximately to the residual angle of internal friction of the soil. Also silt, marl and stiff clay have been utilized (e.g. Tatsuoka et al, 1986; Wichter et al, 1986).

One of the first application of fabric as reinforcement in soil was probably in France in 1971 where the method was used for a motorway (A15). In the United States, fabric was first used as reinforcement in soil in 1974 by the U.S. Forest Service in Oregon State. Bell and Steward (1977) have investigated both model and full-scale fabric reinforced walls. An experimental wall has been constructed and tested relatively early by the New York State Department of Transportation. Also the Colorado Division of Highways has built an experimental fabric reinforced wall (Bell et al, 1983). In Australia, a 20 m long fabric reinforced wall with a maximum height at 1.8 m has been constructed in Sidney by the N.S.W. Public Works Department. In Sweden, fabric reinforced model walls have been tested by Lindskog et al (1975), Broms

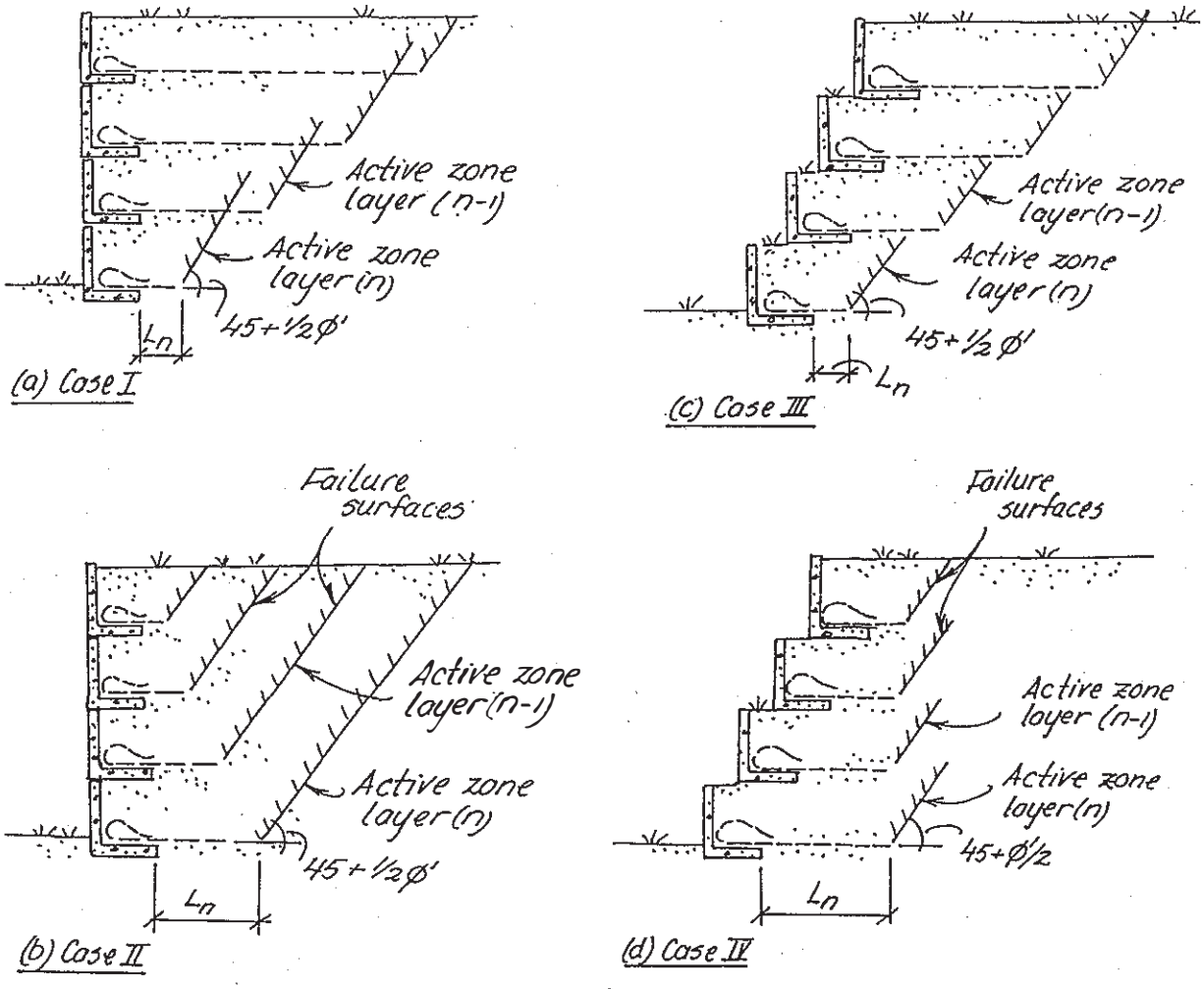

Fig. 12 Fabric reinforced retaining wall (failure mechanisms)

(1975), Davidson and Ekroth (1975) and by Holtz and Broms (1977). In Germany Wichfer et al (1986) have investigated a 4.8 m high fabric reinforced wall. Extensive testing of fabric reinforced walls have also been carried out in England by e.g. John (1986).

There are four basic cases of fabric reinforced retaining walls as illustrated in Fig 12 depending on the length of the fabric reinforcement and the location of the L-shaped elements. In Fig 12a (Case I) the length of the geofabric behind the vertical wall decreases with depth. This variation of the length corresponds usually to the shape of the excavation required for the construction of a fabric reinforced wall. The volume of soil, the active zone, which is affected when the wall fails by sliding along the base of the different layers is also shown in the figure. When sliding occurs along the bottom layer all the overlying layers will be affected. The failure surface will in this case be step-shaped and follow the underside of the overlying fabric layers as shown.

In Fig 12b (Case II), the length of the fabric increases with depth. In this case the volume of soil affected by the sliding will not be affected by the overlaying fabric layers. For the bottom layer the inclination of the failure plane that extends up to the ground surface is approximately ($45^{\circ} + \phi'/2$). It should be noted that the shape and the inclination of the failure surface is affected somewhat by friction resistance along the wall and by the lateral deformations of the wall. It is proposed that this layer should be designed to resist the total active Rankine earth pressure for the full height of the wall neglecting the wall friction.

In Fig 12c and 12d (Cases III and IV) are shown sloping walls where the L-shaped elements are offset with respect to one another. The slope reduces considerably the lateral earth pressure acting on the wall. The length of the reinforcement decreases with depth in Fig 12c (Case III). In this case it is important to consider separately the stability of each row of elements. In Fig 12d (Case IV) the length of the fabric in the different layers increases with depth so that the slip surfaces generated by the different layers overlap.

4.2 Stress Distribution

A section through a fabric reinforced wall is shown in Fig 13. The lateral earth pressure acting on the wall elements will be small since part of the total lateral earth pressure is resisted by the fabric. The reduction of the lateral earth pressure by the fabric reinforcement which is affected by the interface friction angle or the interface cohesion along the fabric can be estimated from the equilibrium of the forces acting on a soil element located between two adjacent fabric layers as shown in the figure. For cohesive soils the lateral earth pressure in the backfill may change with time since it is affected by the porewater pressures in the soil. The undrained shear strength of the soil is normally used during the construction while the effective angle of internal friction (ϕ') as determined from e.g. drained triaxial or direct shear tests is applied for the long term conditions. A considerable increase of the force in the fabric reinforcement can occur during a heavy rainstorm when the porewater pressure in the soil increases (e.g. Tatsuoka et al, 1986).

The friction resistance along the fabric (f) will for a granular soil be proportional to the effective normal pressure (σ_v').

$$f = \sigma_v' \tan \alpha\phi_a' \qquad (8)$$

where $\tan \alpha\phi_a'$ is the coefficient of interface friction of the soil with respect to the fabric. It has thus been assumed in Eq (8) that the relative displacement between the fabric and the soil will be sufficient to mobilize fully the peak interface friction resistance ($\alpha\phi_a'$). For a woven fabric ($\alpha\phi_a'$) will correspond to (ϕ_d') the effective interface friction angle of the soil (eg. Holtz, 1977, 1985). For a non-woven material $\alpha\phi_a'$ can be less than ϕ_a' depending on the large deformation required to mobilize the peak interface friction (Chandrasekaran, 1988).

For a cohesive soil the resistance along the fabric is related to the undrained shear strength c_u as

determined by triaxial tests (UU-tests), field vane tests or unconfined compression tests.

$$f = \alpha c_u \qquad (9)$$

where α is a reduction factor. For stiff clays a value of 0.4 to 0.6 is proposed.

The stress distribution along the reinforcement can then be estimated as illustrated in Fig 13 as discussed by Broms (1978). The friction resistance (f) increases the lateral confining pressure on a soil element located between the two fabric layers from σ_h' at the distance x from the L-shaped elements to $(\sigma_h' + \Delta\sigma_h')$ at $(x + \Delta x)$. At equilibrium

$$2 f dx = D d\sigma_h' \qquad (10)$$

where f is the friction resistance and D is the spacing of the fabric layers. It has thus been assumed that the resulting friction force (2fdx) is distributed uniformly over the height D between two adjacent fabric layer. It should be noted that the vertical and the lateral earth pressure acting in the soil σ_v' and σ_h', are related for granular soils through the lateral earth pressure coefficient K_{av} ($\sigma_h' = K_{av}\sigma_v'$) which is somewhat larger than the Rankine coefficient of active earth pressure (K_a). The stress conditions in the soil just at the fabric corresponds to the earth pressure coefficient K_b [$K_b = 1/(1 + 2 \tan^2\phi_a')$] while at the centre halfway between two layers the stress conditions will be governed by the Rankine coefficient of active earth pressure K_a. It is, therefore, proposed to use an average value K_{av} in the calculations, $K_{av} = 1/2 (K_a + K_b)$].

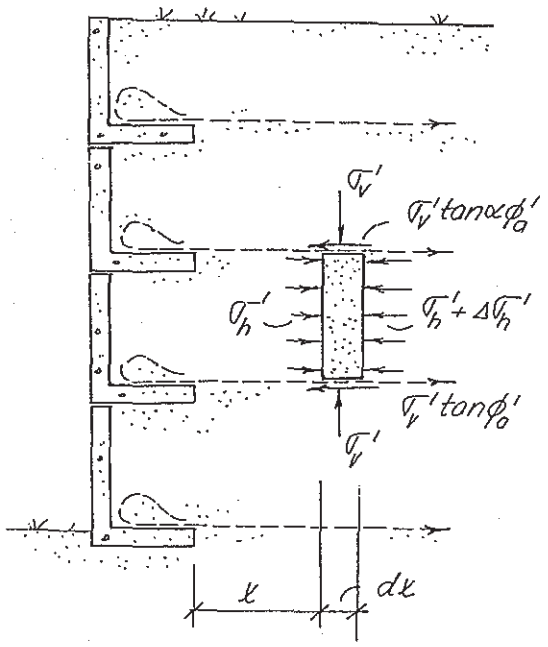

Fig.13 Stress distribution in fabric reinforced soil

From Eqs (8) and (10)

$$d\sigma_v' = \frac{2\,\sigma_v' \tan\alpha\phi_a'}{DK_{av}}\,dx \qquad (11)$$

The solution of this differential equation is

$$\sigma_v' = \sigma_{vo}'\, e^{\frac{2\,x \tan\alpha\phi_a'}{DK_{av}}} \qquad (12)$$

where σ_{vo}' is the bearing capacity at the backface of the wall and x is the distance from the wall.

The bearing capacity of the fabric reinforced wall thus increases rapidly with increasing distance from the wall as illustrated in Fig 14, where the bearing capacity σ_v' has been calculated for $\phi_a' = 30^o$, 35^o and 45^o. The calculated relative bearing capacity will increase ten times at a distance of 0.43D, 0.63D and 0.93D from the wall when the interface friction angle ϕ_a' is 40^o, 35^o and 30^o, respectively. Thus a relatively short distance is required to develop the tensile resistance of the fabric. The face elements can therefore be designed to resist a lateral earth pressure which is considerably smaller than the Rankine active earth pressure.

The corresponding equation for a cohesive soil is

$$d\sigma_v = \frac{2\alpha c_u}{D}\,dx. \qquad (13)$$

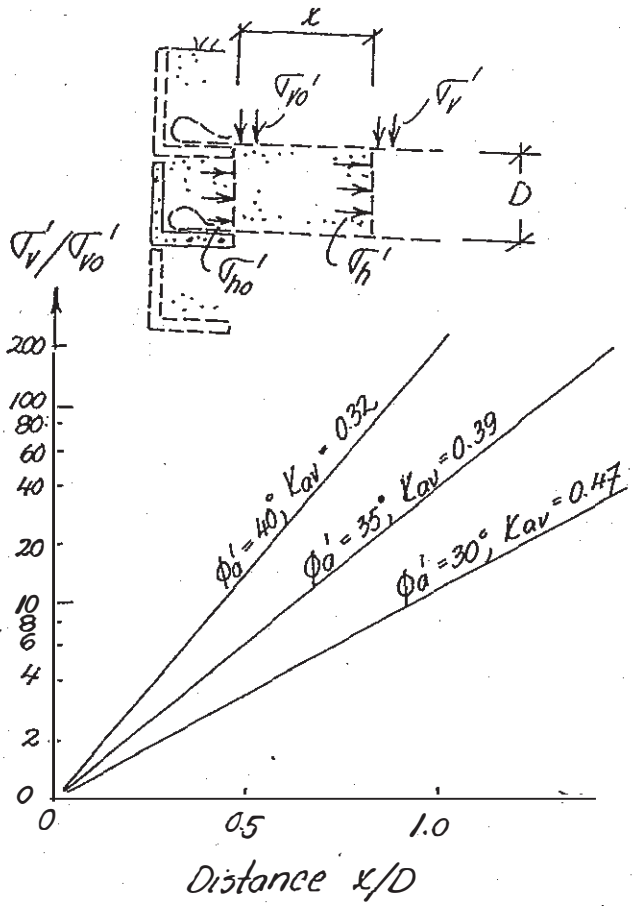

Fig.14 Increase of σ_v'/σ_{vo}' and σ_h'/σ_{ho}' with increasing distance x/D from the face of the retaining structure

The solution of this differential equation is

$$\sigma_v = \frac{2ac_u x}{D} + \sigma_{vo} \qquad (14)$$

where σ_{vo} is the bearing capacity of the wall at the backface of the wall elements. Thus the bearing capacity increases linearly with increasing distance from the wall. This increase is less than that for a granular fill.

4.3 Design of Wall Elements

In Fig 15 is shown the stress conditions just at the backface of the L-shaped elements. For a granular material the equivalent confining pressure is there equal to $\sigma_{ho}' = 2aD\rho \tan\phi_a'$ due to the friction resistance of the soil contained in the elements. At e.g. a = 1.0, D = 1.5 m, ρ = 20 kN/m^3 and ϕ_a = 35° the equivalent confining pressure σ_{ho}' is 42.0 kPa. The corresponding bearing capacity of the soil σ_{vo}' is $K_p\sigma_{ho}'$ or 77.5 kPa at K_p = 3.69. This bearing capacity corresponds approximately to the weight of a 8 m high fill at ϕ' = 35°. Thus the friction alone is not sufficient to prevent failure of the wall by slippage along the reinforcement if the height of the wall exceeds 5 to 10 m depending on the shear strength of the soil and the shape of the elements. It is therefore necessary to bolt or to glue the fabric to the face elements. Another possibility is to fold the fabric as illustrated in Fig 16a so that the force in the fabric can be transferred to the soil. The face elements can be made relatively light since the lateral earth pressure is low. It is proposed that the stem should be designed to resist a

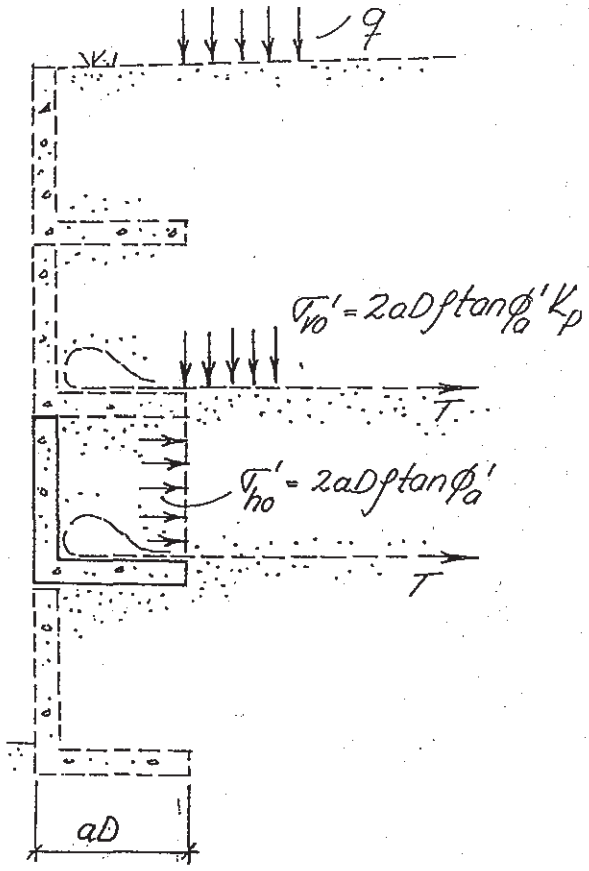

Fig.15 Stress conditions at face elements

lateral earth pressure equal to ($K_a\sigma'_v$ - $a\rho D \tan \phi'_a$).

The construction of the wall is greatly simplified if the fabric if folded as shown in Fig 16a and not connected to the wall. The main disadvantage with this method is the relatively large deformations required to mobilize the tensile strength of the fabric. Compaction of the granular material around the folded fabric is essential in order to reduce the lateral deformations as much as possible. The folds can be filled with coarse sand or gravel in order to improve the drainage since an excess pore water pressure will increase the lateral earth pressure.

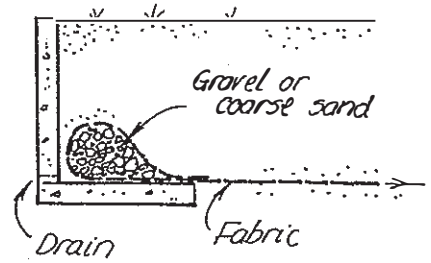

(a) Folding of fabric

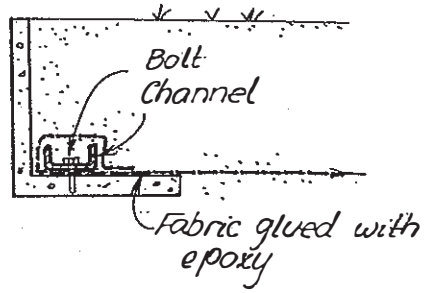

(b) Anchoring of fabric

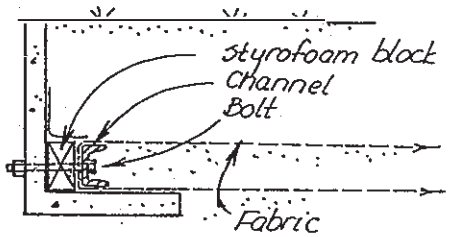

(c) Preloading of fabric

Fig.16 Anchoring of fabric

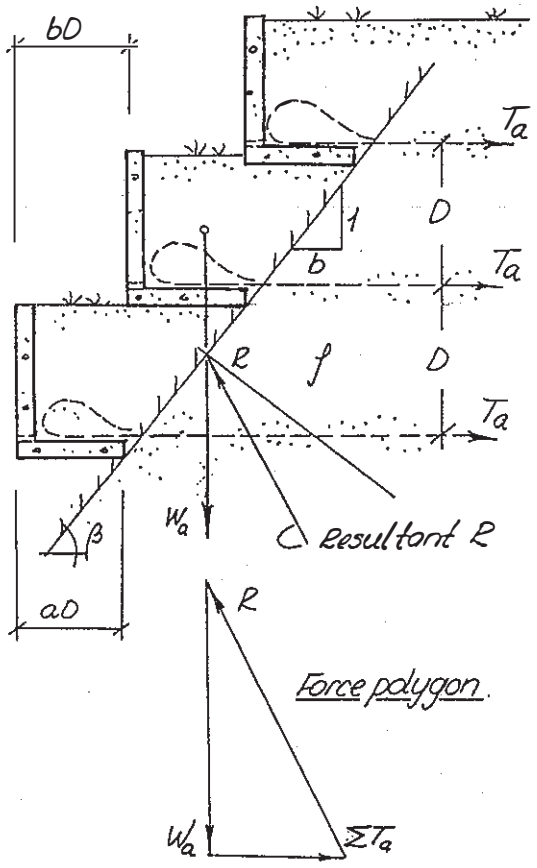

Fig.17 Stability of face elements

The fabric has been glued and bolted to the face elements in Fig 16b. The deformations required to mobilize the tensile strength of the fabric is in this case small. A possible disadvantage with this method is that a damaged wall element is difficult to repair.

The fabric can be preloaded with the arrangement shown in Fig 16c in order to reduce the lateral displacement of the wall elements caused by creep in the fabric. This wall will be relatively easy to repair.

The design of the L-shaped face elements for a sloping wall is illustrated in Fig 17. The fabric will prevent sliding of the elements along an inclined failure surface which corresponds to the average slope (b) of the wall as shown. The average slope depends on the offset of the elements (bD) and on the spacing (D) of the

fabric layers.

The average horizontal thickness of this zone is (aD + 0.5bD) where aD is the width of the base of the L-shaped elements. Each fabric layer had to prevent a block with a mass W_a from sliding which can be estimated from

$$W_a = (a + 0.5b)\, D^2 \rho \qquad (15)$$

The force T_a in the fabric which is required to prevent the L-shaped elements from sliding is then equal to

$$T_a = W_a \tan(\beta - \phi) \qquad (16)$$

This force decreases with increasing inclination of the slope as can be expected. At e.g. $\beta = 60^o$ and $\phi = 30^o$ then $T_a = 0.58\ W_a$. The force in the fabric depends also on the height of the elements (D). At D = 1.5 m, ρ = 20 kN/m^3 and W_a = 43.0 kN/m then T_a = 24.9 kN/m. This force in the fabric had to be transferred to the L-shaped elements and to the soil.

The friction resistance (F_a) of the fabric within the elements is $2aD^2\rho\tan\phi_a'$. At, for example, aD = 1.0 m, ρ = 20 kN/m^3, D = 1.5 m and $\phi_a' = 30^o$ then F_a = 34.3 kN/m. The corresponding factor of safety (F_s) is 1.38 (34.3/24.9) which is not sufficient. It is desirable that the factor of safety should be at least 1.5 to 2.0. The factor of safety can be increased by folding or bolting the fabric to the elements (Fig 16a and 16b).

The L-shaped elements can even be replaced entirely by folding the fabric as illustrated in Fig 18. The different fabric layers will in this case function as a series of sandbags. The resulting tension in the fabric is governed by the radius (R) of the folds and by the total overburden pressure ($H\rho$+q) where H is the height of the wall and q is the surcharge load. The maximum tension in the fabric in the bottom layer can then be calculated from

$$T_b = K_a\, (H\rho + q)R \qquad (17)$$

where K_a is the coefficient of active earth pressure. At H = 10 m, ρ = 20 kN/m^3, K_a = 0.3 and R = 0.3 m then T_b = 19.8 kN/m. Thus a relatively high tension can develop in the bottom layer of the folded fabric of a high wall. It has been assumed in the derivation of Eq (17) that the shear resistance of the soil is fully mobilized. The tension in the fabric can be reduced by filling the folds with a granular material with a high angle of internal friction such as coarse sand or gravel or by decreasing the radius of the folds.

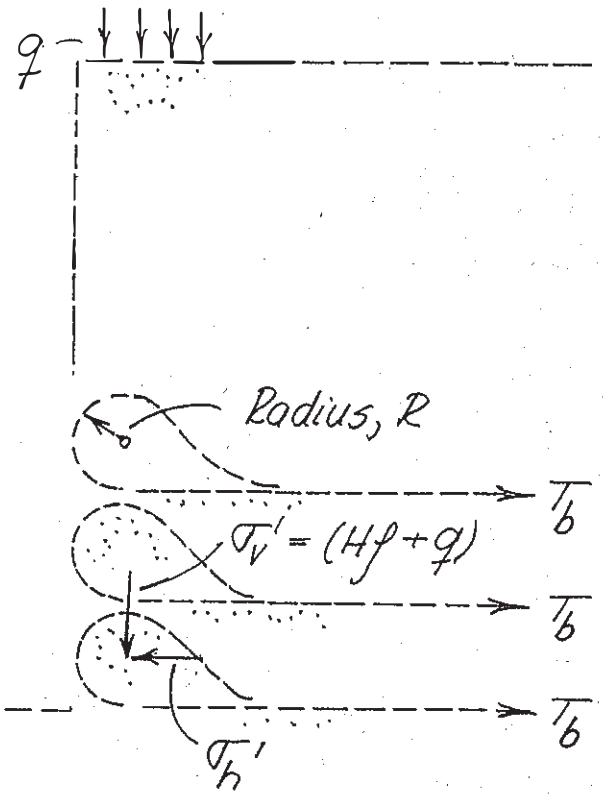

Fig.18 Design of folds

The fabric had to be protected in this case against direct sunlight by spraying the surface with shotcrete or by a precast concrete wall as shown in Fig 19. The required thickness of the shotcrete cover is 50 to 75 mm. Wire mesh can be used as reinforcement. Experience indicates that shotcrete cover can withstand relatively large differential settlements when reinforced. The precast concrete elements can be made very light since their only function is to protect the fabric against direct sunlight and vandalism. The face elements can be anchored to the fabric with steel or

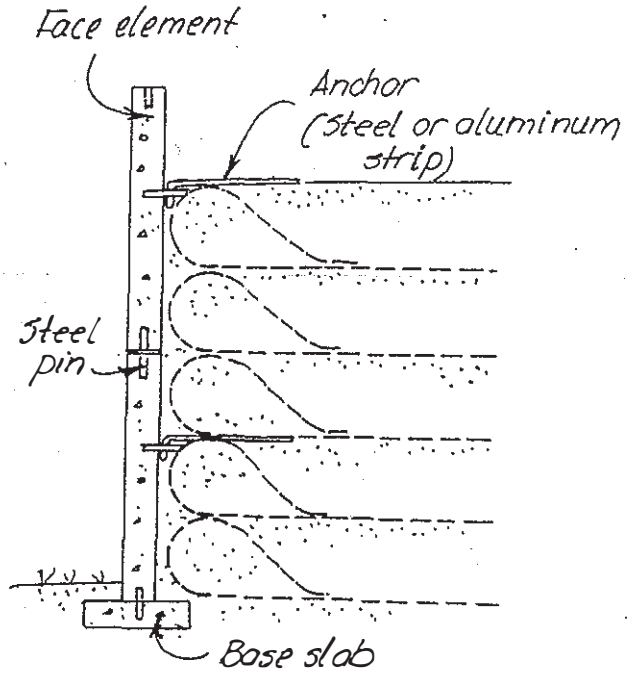

Fig.19 Light concrete slabs as face elements

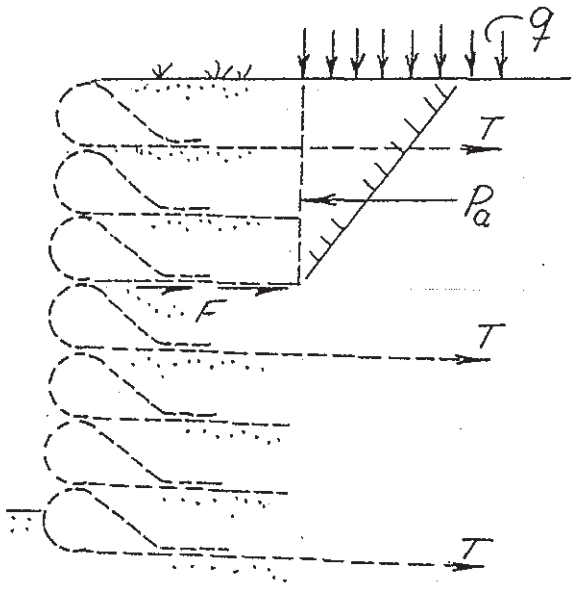

Fig.20 Required length of fabric reinforcement

aluminium straps. The space between the wall and the face elements could be filled with loose sand to eliminate any voids behind the wall. The sand will also prevent loss of material from the folds in case the fabric ruptures or tears locally. The resulting lateral pressure acting on the face elements will be low due to arching.

It is not necessary to extend all the fabric layers the full length if the tensile resistance of the remaining layers is sufficient especially in the upper part of the wall as illustrated in Fig 20. However, the stability of each level had to be checked with respect to a failure surface extending below the fabric reinforcement as shown.

4.4 Design of Fabric Layers

The axial force in the geofabric depends mainly on the inclination of the wall and on the length of the fabric reinforcement (Cases I, II, III and IV). In Case I, where the length of the fabric reinforcement decreases with depth and the wall is vertical the stress distribution in the geofabric will be as shown in Fig 21a. For a vertical wall the inclination of the critical failure surface is usually assumed to be $(45 + \phi'/2)$. In France, a spiral shaped failure surface is often used which can be approximated by two straight lines. The difference between the two methods is small.

The force in the fabric will increase with increasing distance from the two ends and reach a maximum approximately where the potential failure surface from the bottom element intersects the different layers. For a vertical wall the tension in the fabric reaches a maximum at a section that is inclined at approximately an angle $(45 + \phi'/2)$ with the vertical. For a sloping wall, the critical section is located further back into the slope.

It is proposed to calculate the axial force in the fabric as shown in Fig 21b. The indicated constant earth pressure distribution for a vertical wall is similar to that proposed by Terzaghi and Peck (1967) for braced excavations. Model tests and observations on instrumented fabric reinforced walls indicate that the force in the fabric

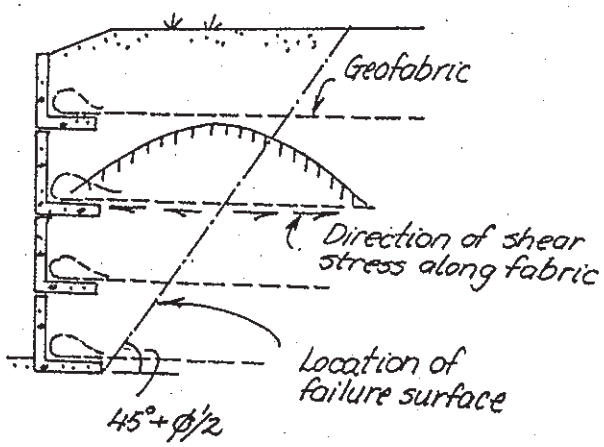

(a) Stress distribution along fabric

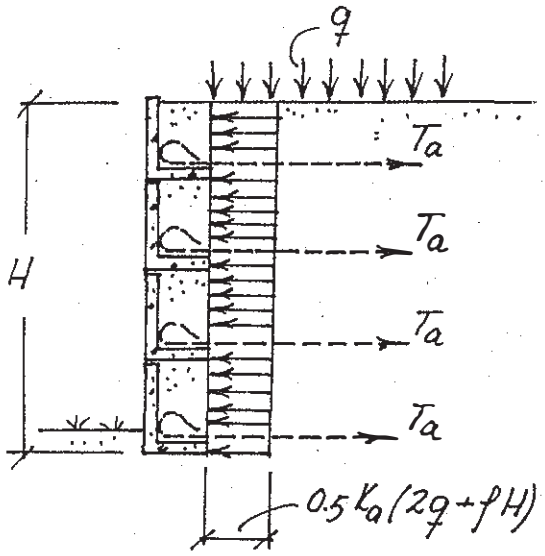

(b) Stress distribution along wall

Fig.21 Design of retaining wall (Case I)

does not increase linearly with depth and that it is approximately constant (e.g. John, 1979, 1986). It is thus proposed that the fabric should be designed for a lateral earth pressure $\sigma'_h = 0.5\ K_a\ (2q + \rho H)$ where H is the total height of the wall, K_a is the Rankine coefficient of active earth pressure and ρ is the unit weight of the backfill material. It is proposed to use the critical state angle of friction in the calculation of the active earth pressure because of the large deformations required to mobilize the resistance of the fabric reinforcement. This corresponds to the residual friction angle at large deformations of the soil. This is a conservative assumption. The total lateral earth pressure is equal to the total active Rankine earth pressure.

Gourc et al (1986) and others have suggested that the vertical displacement of the fabric at the critical failure surface in the backfill could also be considered in the calculations. This displacement will increase the stabilizing effect by the fabric. It is proposed that this effect should not be taken into account in the design since a relatively large displacement is required to develop the maximum resistance of the fabric.

The total lateral force at a section though the backface of the L-shaped elements will be resisted by the fabric reinforcement and by the friction along the base of the wall. The required spacing of the fabric (D) for a vertical wall can be calculated from the relationship.

$$D = \frac{T_a}{0.50\ K_a\ (2\ q + \rho H)} \qquad (18)$$

where T_a is the allowable long term tension in the fabric and q is the unit load acting on the surface of the backfill.

The design of the fabric reinforcement when the length of the layers decreases with depth is shown in Figs 22a and 22b. The different fabric layers should be designed to resist a tension force that corresponds to the active Rankine earth pressure as illustrated in Fig 22a. Each fabric layer had to resist the total lateral earth pressure acting above that layer as shown in Fig 22b. The bottom layer should be designed to resist a lateral force that corresponds to the total active Rankine earth pressure for the full height of the wall.

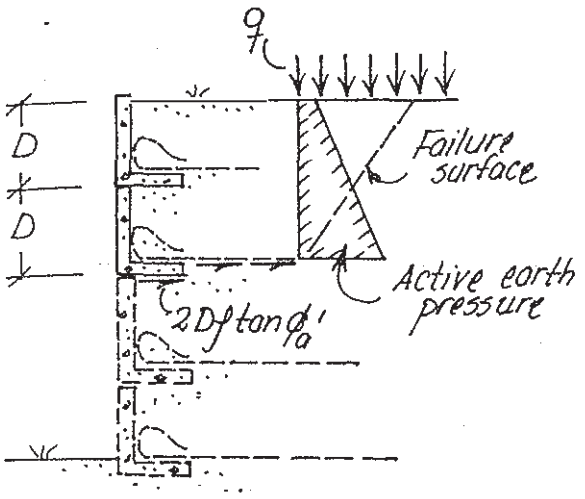

(a) Local failure

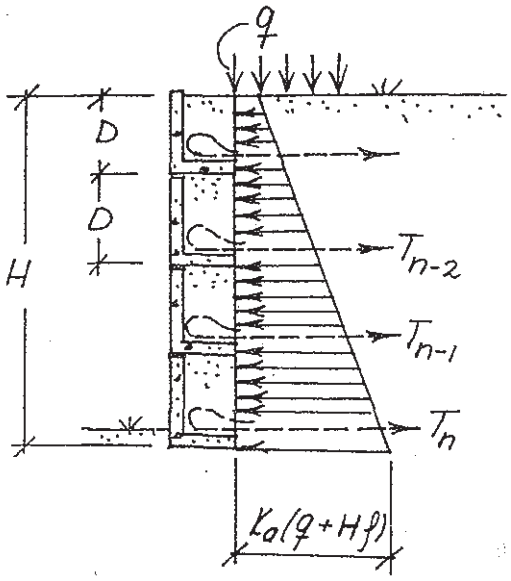

(b) Stress distribution along wall

Fig.22 Design of retaining wall (Case II)

The force in the fabric for a sloping wall is illustrated in Fig 23a and 23b (Case III). The fabric reinforcement should prevent failure along different possible failure surfaces in the soil. When the ground water level is low and the effective cohesion (c') is equal to zero then the soil located above an inclined plane steeper than φ' will be unstable. This plane thus governs the required length of the fabric.

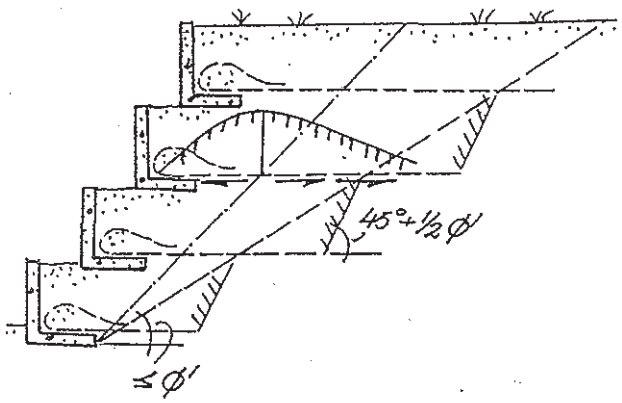

(a) Stress distribution along fabric

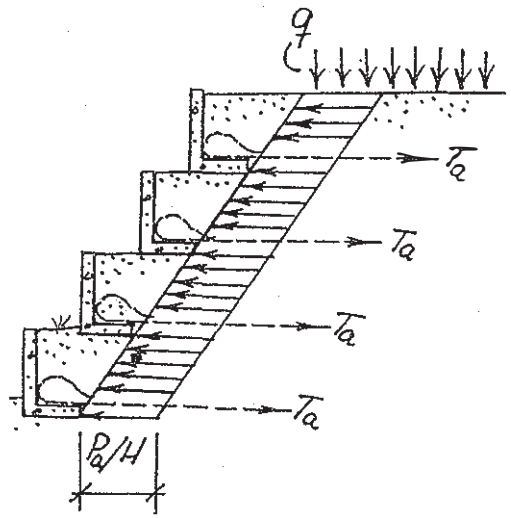

(b) Stress distribution along wall

Fig.23 Design of retaining wall (Case III)

The force in the fabric (T_n) will vary along the length and with the inclination of the failure plane. This force can be calculated from the weight of the soil mass (W_n) above the assumed failure plane and from the direction of the resultant (R) to the normal force and the shear force along the failure plane as shown in Fig 24. At equilibrium

$$\Sigma T_n = W_n \tan (\beta - \phi') \qquad (19)$$

where β is the inclination of the assumed failure plane. The total tension in the fabric $\Sigma T/H^2\rho$ has been plotted in Fig 25 as a function of the inclination of the slope (b) for different values of the effective angle of internal friction ϕ' of the soil. It can be seen from the figure that the total force in the fabric reinforcement decreases rapidly with decreasing inclination of the slope (b) and with increasing angle of internal friction as shown in Fig 25. At e.g. b = 0.5 which corresponds to a slope of 63.4 degrees $\Sigma T_n/H^2\rho$ = 0.03. The total required

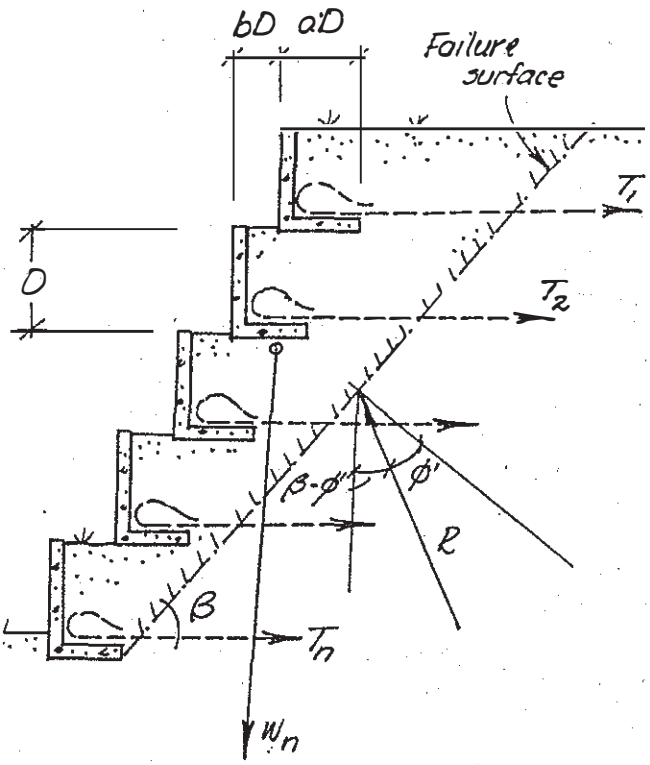

Fig.24 Stability of a sloping wall

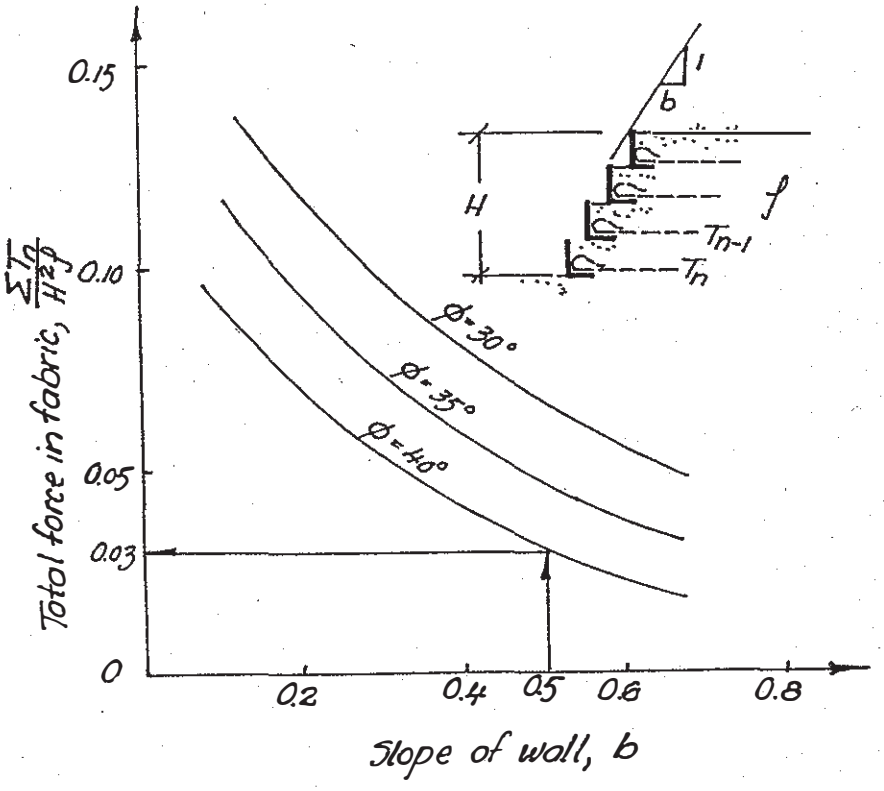

Fig.25 Force in fabric reinforcement for a sloping wall

anchor force ΣT_n is 60 kN/m at $\phi' = 40^o$, H = 10 m and ρ = 20 kN/m^3.

It is proposed to distribute the total lateral earth pressure uniformly between the different fabric layers. When one layer becomes overloaded a redistribtion of the applied load will occur due to the ductility of the fabric. At a vertical spacing of 2 m the maximum tension in each layer is 12 kN/m (60/5) since there are five layers in this case. At b = 0.3 which corresponds to a slope of 73.3 degrees, $\Sigma T_n/H^2\rho = 0.097$. At $\phi' = 30^o$, H = 10 m and ρ = 20 kN/m^3, ΣT_n = 194 kN/m. The maximum tension in each layer is 38.8 kN/m (194/5).

The stress distribution along a sloping wall when the length of the reinforcement increases with depth is shown in Fig 26. Each layer should to be designed to resist a lateral earth pressure that corresponds to the height of the wall above that layer. For the second layer the height is 2D as shown in Fig 26. Fig 25 can be used to estimate the total lateral force. The height 2D should be used instead of H in this case.

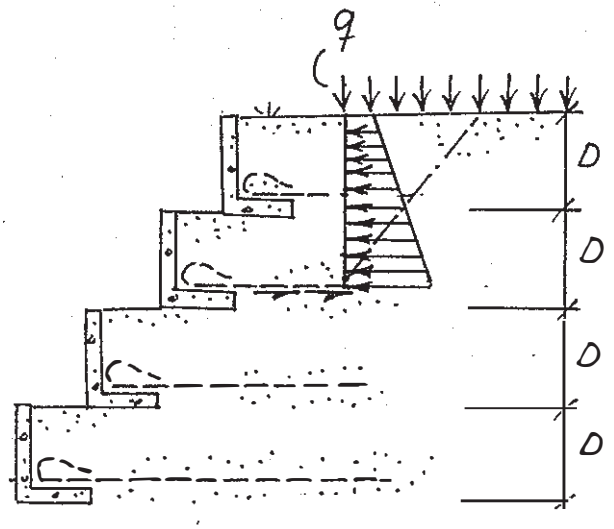

Fig.26 Required tensile strength of fabric reinforcement-sloping wall

4.5 Length of Fabric Reinforcement

The required length of the fabric reinforcement can be determined as illustrated in Fig 27. The length should be sufficient so that the average slope of the failure surface extending beyond the fabric corresponds to the effective angle of internal friction of the soil (ϕ'). In Figs 27a and 27b are shown the required length for a vertical wall in the case the length of the fabric decreases or increases with depth, respectively (Cases I and II). The fabric reinforcement forces the soil and the wall located above the failure surface to move as a unit. This block of soil will be stable as long as the average slope of the failure surface is less than ϕ' when the effective cohesion of the soil (c') is small. This is a conservative assumption since the effective cohesion increases the stability. It is proposed to neglect the effective cohesion for permanent structures since the effective cohesion decreases with time and is very difficult to determine.

The face of the wall is sloping in Cases III and IV. The length of the fabric layers can either decrease or increase with increasing depth as illustrated in Figs 27c and 27d, respectively. The potential failure surface for the bottom layer is also indicated in the figure and the corresponding active zone. Failure will in this case occur along the base of the bottom layer. The failure surface will extend from the end of the fabric layers up to the ground surface. The inclination is (45^o + 1/2 ϕ') when the wall friction is small and can be neglected.

The length of the different layers is short in Cases II and IV compared with Cases I and III but the force in the fabric will be larger. Cases I and III will in general be more economical for cut slopes where the costs for the excavation of the soil is large compared with the cost for the fabric. Cases II and IV where the length of the fabric reinforcement increases with depth is normally more economical for fill slopes where excavation is not required. High strength fabric or several layers might be required in the bottom layer in order to resist the high lateral force caused by the total active earth pressure for the full height of the wall.

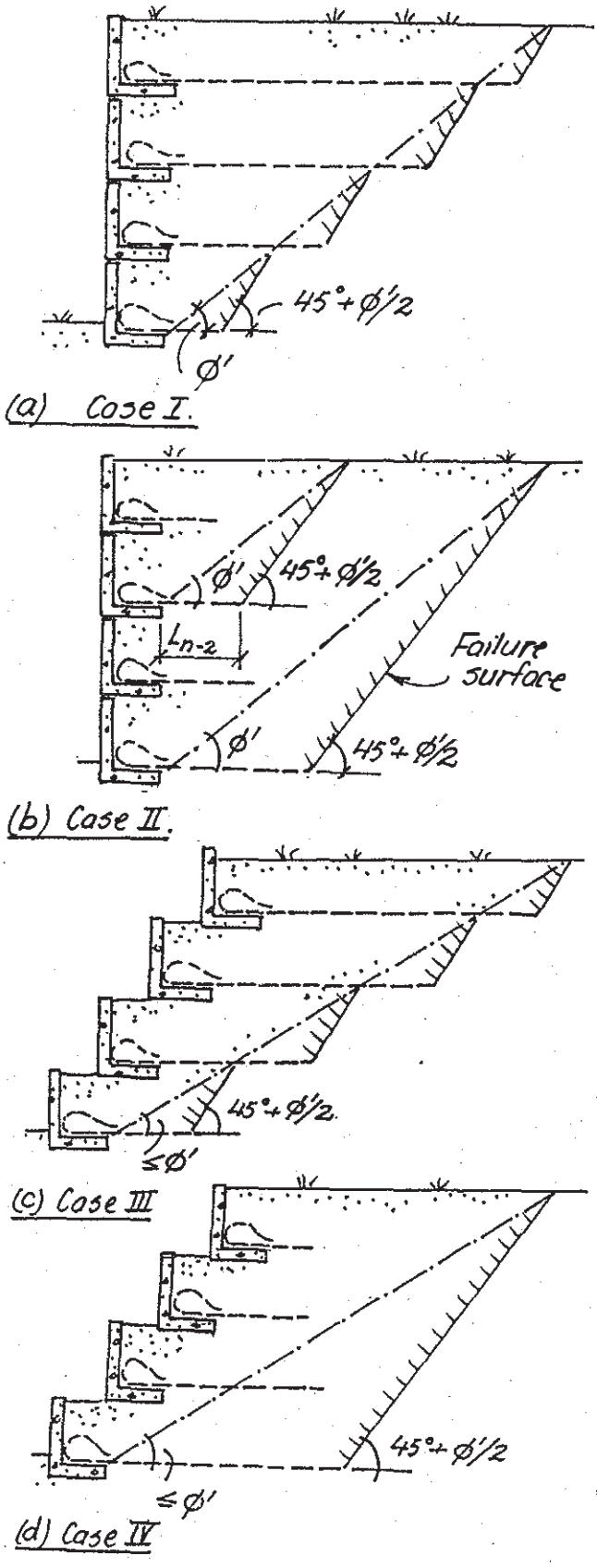

Fig. 27 Length of reinforcement

4.6 Bearing Capacity

It is also important to check that the bearing capacity of the soil below the wall is sufficient as illustrated in Fig 28a. The total weight (W_a) of the wall and of the soil contained in the elements will mainly be carried through the vertical stems of the L-shaped elements. The load will be vertical because of the fabric reinforcement that resists the lateral earth pressure acting on the wall.

The bearing capacity of the wall elements should also be checked when the wall is sloping as illustrated in Fig 28b. The load W_b which is transferred to the soil will be small in this case since the fabric has been designed to carry the weight of the L-shaped elements and the soil contained in the elements. It is also important to check the bearing capacity of the soil for the full height of the embankment. This can be done by assuming that the failure takes place along a circular slip surface below the elements. It should be noted that the fabric reinforcement improves the bearing capacity of the underlying soil also for this case.

4.7 Lateral Displacements

The lateral displacement of a fabric reinforced wall is often the largest at the top of the wall. The displacement at the bottom is usually small even close to failure. The lateral displacement is generally small at working loads. The maximum displacement increase rapidly as the ultimate capacity of the wall is approached.

The lateral displacements depend to a large extent on the type of fabric used, woven or non-woven. The maximum displacement is also affected by creep of the fabric material and thus by the ground temperature which is normally relatively constant except close to the wall. The lateral displacement caused by creep increases approximately with log (t). The creep of polypropylene fabric is usually larger than that of polyester but the initial deformation is smaller. The creep of polyaramid is very low. It is therefore important that creep tests are carried out over a range of temperatures.

The finite element method (FEM) has been used with some success to predict

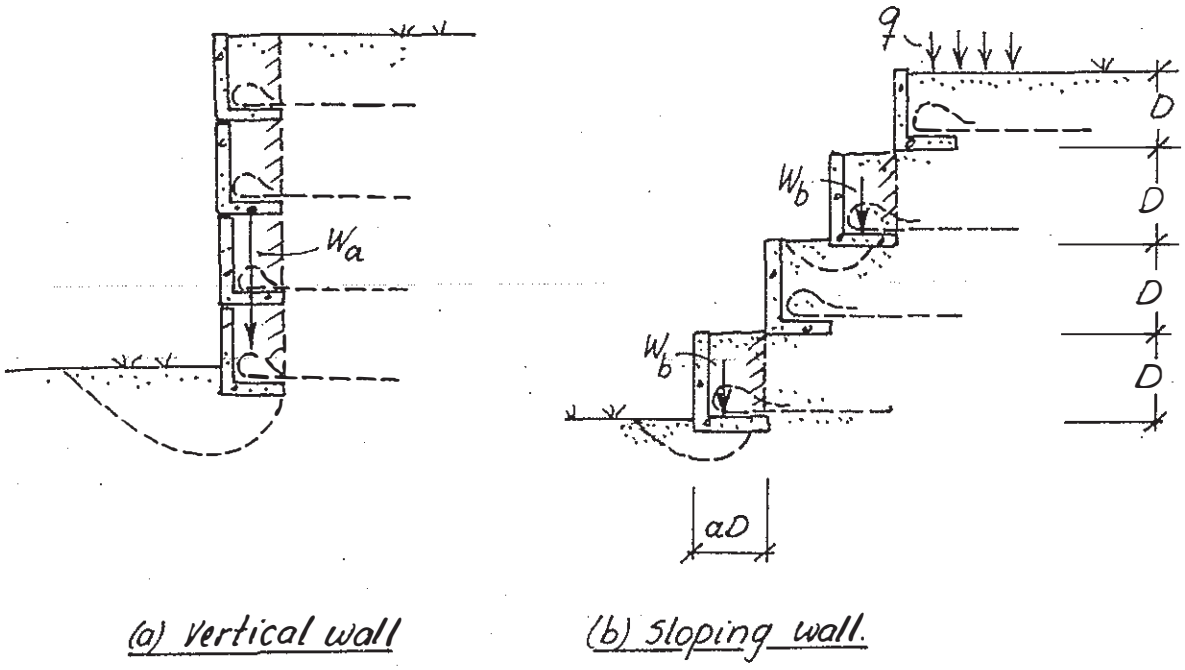

Fig.28 Bearing capacity of wall elements

the lateral displacements at working loads using a non-linear stress-strain relationship for the soil. The accuracy of the method depends mainly on how accurate the deformation properties of the soil (E and ν) and of the fabric can be determined.

It is proposed to estimate the lateral displacement of a fabric reinforced wall from the load distribution in the fabric. The maximum tension in the fabric T_{max} can be estimated as described earlier by e.g. the Rankine earth pressure theory. This maximum force corresponds to an axial strain ϵ_{max} in the fabric which can be determined from confined tension tests. At working loads the axial strain may be only 40 to 60% of the strain determined from unconfined tension tests.

The tension in the fabric will decrease on both sides of the critical failure surface through the backfill. The reduction depends on the interface friction resistance ($\alpha\phi_a'$) and on the effective overburden pressure $\sigma_v'(= nD\rho)$.

The required length to reduce the tension in the fabric to zero is $T_{max}/nD\rho\tan\phi_a'$, where nD is the depth below the surface and ρ is the unit weight of the soil. At a linear variation of the strain distribution in the fabric the maximum lateral deformation of a vertical or sloping wall (δ_{max}) when the length of the fabric decreases with depth (Cases I and III) can be estimated from

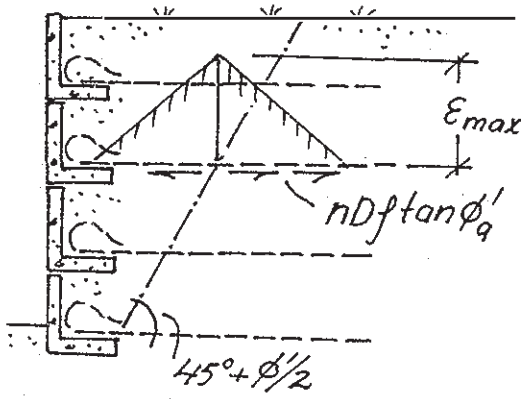

Fig.29 Strain distribution in fabric

$$\delta_{max} = \frac{\epsilon_{max} \cdot T_{max}}{nD\rho\tan\phi_a'} \qquad (20)$$

In the case the load distribution is uniform the lateral deformations will decrease approximately linearly with depth since the total overburden pressure ($nD\rho$) increases with depth. Close to the surface δ_{max} = 144 mm at n = 1, D = 1.5 m, ρ = 20 kN/m^3, ϕ'_a = 30 degrees, T_{max} = 50 kN/m, ϵ_{max} = 5%. The corresponding lateral deformation at 6 m depth (n = 4) is 36 mm.

In the calculation of the lateral deflection of a vertical or an inclined wall when the length of the fabric increases with depth the lateral deformation of the soil behind the fabric reinforcement must also be considered. This deformation is governed by the lateral displacement of the underlying layers. The lateral displacement of the bottom layer ($\delta_{n,max}$) can be estimated from Eq (20). The corresponding lateral displacement for the following layer $\delta_{n-1,max}$ is

$$\delta_{n-1,max} = \delta_{n,max} + \frac{\epsilon_{n-1,max}\, T_{n-1,max}}{(n-1)\, D\rho \tan \phi'_a} \qquad (21)$$

Since the force T_n increases linearly with depth when the spacing D is constant, then the lateral deformation as calculated by Eq (21) will also increase linearly with depth.

The lateral deformation required to develop the maximum resistance of a non-woven material is large compared with that of a woven fabric and the resulting deformation may be excessive for most structures. However, the behaviour of non-woven geotextiles is stiffer than indicated by unconfined tension tests when used as reinforcement in soil. The deformations can also be reduced by prestretching (Finnigan, 1977), by reducing the stress level in the fabric or by increasing the number of layers. The wall can often be inclined backwards, thereby reducing the lateral earth pressure acting on the wall. It is also possible to make allowance for the relatively large deformations of the fabric in the design. Fabric reinforced walls can often move considerably without any signs of distress.

4.8 Settlements

Relatively large settlements can normally be accepted, 100 to 200 mm, without any detrimental effects on the wall because of the large flexibility of the fabric reinforcement. The face elements can also tolerate large settlements depending on the size and shape of the elements. The settlements of a fabric reinforced wall is caused by

* the settlement of the fill which can be reduced by compaction and by
* the settlement of the soil below the fill and the wall. There may be soft clay or silt layers below the fill which can increase the settlements considerably.

The settlements below the fill and the wall can be reduced with embankment piles, stone or gravel columns or by replacing the compressible soil strata with granular material (sand or gravel).

4.9 Construction of Fabric Reinforced Walls

The following sequence is normally followed in the construction of a fabric reinforced retaining wall

a. Before the beginning of the construction of the wall itself and the placement of the fill behind the wall the area should levelled and the soil compacted by e.g. a 3 to 5 tonne vibratory roller to at least 90% relative compaction as determined by the modified Proctor compaction tests (modified AASHO) in order to reduce the settlements of the soil below the fill. The area should be properly drained. Drain pipes might be required. Surface water should be channelled to collector drains.

b. The bottom row of the prefabricated L-shaped elements can then be placed on the compacted surface and a 0.3 m thick layer of granular fill is spread out behind the concrete elements and compacted. The percentage of fines (< 0.06 mm) in the granular material should be less than 10 to 15%.

c. Thereafter the first layer of fabric is rolled out on the compacted fill.

A string of gravel or coarse sand is placed on the fabric next to the wall for drainage. The fabric is folded over the gravel or sand layer as protection and to anchor the fabric. It is important that sufficient length of fabric is available for the folding.

d. Additional fill can then be placed on the fabric and compacted in 0.3 to 0.5 m lifts up to the top of the concrete elements. The maximum thickness of each layer depends on the available compaction equipment (plate vibrators or vibratory rollers). It is possible to use also a silty or a clayey material as fill except next to the fabric reinforcement. The thickness of the layers should then be reduced. The interface friction angle may otherwise be too low. The compaction should be done in the direction away from the concrete elements in order to pretension the fabric and to reduce the lateral deformations of the wall. The compaction next to the elements should be done in small lifts with a light plate vibrator. Otherwise the concrete element might be displaced during the compaction.

e. The next level of the L-shaped elements is placed on the compaction fill after the fill has been brought up to the top of the underlying elements. Additional fill can be placed behind the concrete elements after the next level of fabric has been rolled out in the same way as described above. Heavy equipment is not required to lift the concrete elements since they are light.

5 EXAMPLE

In the design of a fabric reinforced retaining wall it is important to consider

* the sliding resistance along different possible slip surfaces,
* the general stability of the wall with respect to a failure surface that extends behind the fabric reinforcement and below the structure (deep seated failure) and
* the bearing capacity of the soil below the wall

The resistance against sliding along the base of the 4 m high fabric reinforced wall shown in Fig 30 depends on the

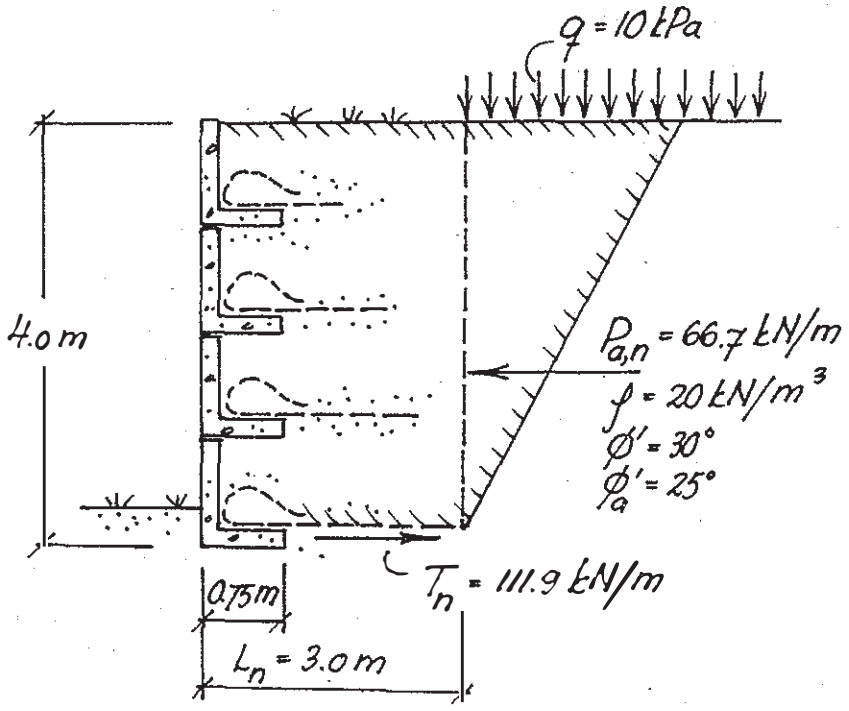

Fig.30 Design of a 4 m high fabric reinforced retaining wall - Sliding along base

length (3 m) of the fabric at the bottom of the wall. The force initiating failure [$P_{an} = 0.5\ HK_a\ (2q + H\rho)$] is governed by the coefficient of active earth pressure K_a, the height of the wall H and the surcharge load q. At H = 4.0 m, K_a = 0.33, q = 10 kPa and ρ = 20 kN/m^3 the force initiating failure is 66.7 kN/m. The force resisting failure ($T_n = W_n \tan \phi_a'$) with respect to sliding along the base is 111.9 kN/m at L_n = 3.0 m, H = 4.0 m, ϕ_a' = 25° and ρ = 20 kN/m^3. The corresponding factor of safety is 1.68 (111.9/66.7) which is considered to be satisfactory. A global factor of safety of 1.5 to 2.0 is usually required.

A high tension force will develop in the bottom fabric layer as the wall slides along the base. The maximum tension in the fabric depends on the friction resistance with respect to sliding along the bottom face of the fabric. Because the length of the fabric beyond the base of the L-shaped elements is 2.25 m, the maximum force in the fabric is 83.9 kN/m (2.25 x 4.0 x 20 x tan 25°)since ϕ_a' is 25 degrees. At a required factor of safety of 2.0 the minimum tensile strength of the fabric should be 167.8 kN/m (2 x 83.9). A maximum allowable load equal to 50% of the short term strength has been recommended for polyester fabric by Jewell and Greenwood (1988). A relatively high factor of safety is also necessary to limit the lateral displacement of the wall. Thus high strength fabric is required in this case in order to force the critical failure surface away from the wall.

The lateral displacement of the bottom layer can be estimated from Eq (20). The displacement thus depends on the maximum force in the fabric, which will be less than 66.7 kN/m (Pa) due to the friction resistance along the base of the L-shaped elements. This friction resistance is estimated to 28.0 kN/m (4 x 20 x 0.75 x tan 25°). At ϵ_{max} = 5%, T_{max} = 38.7 kN/m, nD = 4 m, ρ = 20 kN/m^3 then $\delta_{n,max}$ = 0.051 m.

Also other possible slip surfaces should be checked as illustrated in Fig 31. The active earth pressure (P_a) initiating failure at the second level of the face element is 20 kN/m. The

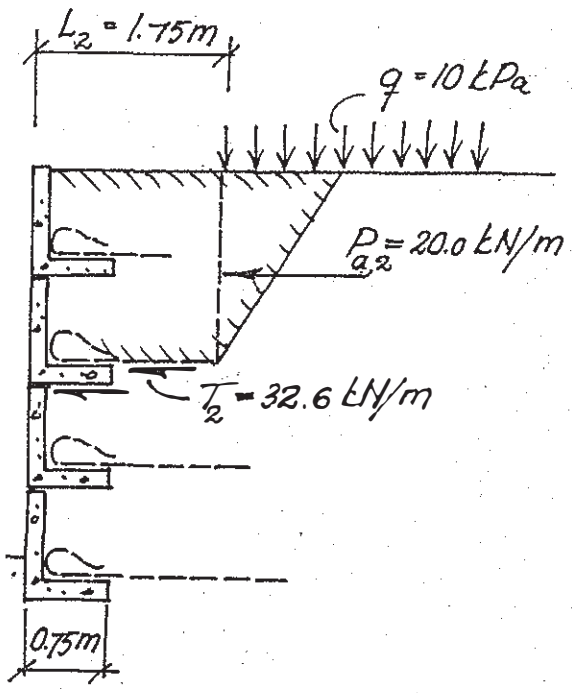

Fig.31 Local stability of retaining wall

force resisting sliding along the base is 32.6 kN/m (2 x 1.75 x 20 x tan 25°). The calculated factor of safety with respect to sliding along the base is 1.63 (32.6/20). This factor of safety is considered to be satisfactory.

The maximum tension in the fabric is estimated to 18.6 kN/m (1.0 x 2.0 x 20 x tan 25°). The required tensile strength of the fabric is thus 37 kN/m (2 x 18.6) at a minimum factor of safety of 2.0. It should be noted that the required tensile strength of the fabric decreases rapidly with decreasing distance below the ground surface.

The bearing capcity of the soil below the base of the L-shaped elements should also be checked. It should be noted that the fabric reinforcement will increase the bearing capacity since the lateral earth pressure is resisted by the fabric. Only the total over-burden pressure had to be taken into account. It is also important to consider the total stability of the wall with respect to a failure surface that extends behind the reinforcement and below the wall.

The fill behind the retaining wall should be carefully drained so that the

excess pore water pressures in the soil will be small and can be neglected. The fabric reinforcement will also function as drainage layers which will reduce further the excess pore water pressures. The fill material should preferably be sand or gravel with a high permeability. It is desirable that the content of silt and clay size particles ($\leq$ 0.06 mm) should be less than 10 to 15%. The L-shaped concrete elements should be provided with drainage holes to relieve any excess pore water pressures in the fill behind the wall. If the pore water pressure increases in the fill during e.g. a heavy rain storm the lateral earth pressurs can be considerably higher than those indicated previously. This can be a problem in areas with a high annual rainfall such as Singapore.

Slotted PVC pipes can also be placed at the bottom of the backfill perpendicular to the wall in order to reduce the excess pore water pressures. The pipes should be connected to the gravel or sand layer just behind the wall.

6 SUMMARY

The application of geofabric as reinforcement in soil for vertical and inclined retaining walls have been reviewed. Geofabric can be used, for example, to reduce the lateral earth pressure on retaining walls or other retaining structures and to increase their stability. Calculation methods based on different possible failure mechanisms are presented in the paper so that the force in the fabric reinforcement can be estimated. The fabric reinforcement had to be designed to resist the total active Rankine earth pressure for the full height of the wall.

7 REFERENCES

Andrawes, K.Z., McGown, A. and Kabir, M.H., 1984. Uniaxial Strength Testing of Woven and Non-woven Geotextiles and Geomembranes, Vol.1, pp 41 - 56.

Bell, J. R. and Steward, J.E., 1977. Construction and Observations of Fabric Retained Soil Walls. Int. Conf. on the Used of Fabrics in Geotechnics, Paris, Vol. I, pp 123 - 128.

Bell, J.R., Barrett, R.K. and Ruckman, A.C., 1983. Geotextile Earth-Reinforced Retaining Wall Tests : Glenwood Canyon, Colorado, Transportation Research Record No 916, pp 59 - 69.

Broms, B.B., 1977. Polyester Fabric as Reinforcement in Soil. Int Conf on the Use of Fabrics in Geotechnics, Paris, Vol I, pp 129 - 135.

Broms, B. B., 1978. Design of Fabric-Reinforced Retaining Structures. Symposium on Earth Reinforcement, ASCE. Annual Convention, Pittsburg, pp 282 - 304.

Chandrasekaran, B., 1988. An Experimental Evaluation of Fabric Strength Properties and Behaviour of Fabric Reinforced Soil, Master of Engineering Thesis, National University of Singapore, 275 pp.

Christopher, B.R., Holtz, R.D. and Bell, W.D. 1986. New Tests for Determining the In-Soil Stress-Strain Properties of Geotextiles. Proc. 3rd Int. Conf. on Geotextiles, Vienna, Austria, Vol. 3, pp 683 - 688.

Colin, G., Mitton, M.T., Carlsson, D.J. and Wiles, D.M., 1986. The Effect of Soil Burial Exposure on Some Geotechnical Fabrics, Geotextiles and Geomembranes, Vol.4, pp 1 - 8.

Davidson, S. and Ekroth, N., 1975. Försök med vävförankrad stödmur, (Tests with retaining walls reinforced with fabric). Royal Institute of Technology, Stockholm, Unpublished Thesis, 43 pp.

Degoutte, G. and Mathieu, G. 1986. Experimental Research of Friction between Soil and Geomembranes or Geotextiles using a 30 x 30 cm Square Shearbox. Proc. 3rd Int. Conf. on Geotextiles, Vienna, Austria, Vol. 4, pp. 1251 - 1256.

El-Fermaoui, A. and Nowatzki, E., 1982. Effect of Confining Pressure on Performance of Geotextiles in Soil. Proc. 2nd Int. Conf. on Geotextiles, Las Vegas, Nevada, Vol. 3, pp 799 - 804.

Finnigan, J.A., 1977. The Creep Behaviour of High Tenacity Yarns and Fabrics Used in Civil Engineering

Applications. Proc. Int. Conf. Use of Fabrics in Geotechnics, Paris, Vol. 2, pp 305 - 309.

Fowler, J., 1982. Theoretical Design Considerations for Fabric Reinforced Embankments. Proc 2nd Int Conf of Geotextiles, Las Vegas, Vol 3, pp 671 - 676.

Gourc, J.P., Ratel, A. and Delmas, P., 1986. Design of Fabric Retaining Walls : The "Displacement Method". Proc. 3rd. Int. Conf. on Geotextiles, Vienna, Vol. 2, pp 289 - 294.

Hausmann, M.R., 1976. Strength of Reinforced Soil. Proc 8th Aust. Road Res. Conf., Vol 8, Sect. 13, pp 1 - 8.

Hausmann, M.R. and Vagneron, J.M., 1977. Analysis of Soil Fabric Interaction. Proc. Int. Conf. on the Use of Fabric in Geotechnics, Paris, Vol 3, pp 139 - 144.

Holm, G. and Bergdahl, U., 1979. Fabric Reinforced Earth Retaining Walls - Results of Model Tests C.R. Coll. Int. Reinforcement des Sols, Paris, pp 53 - 58.

Holtz, R.D., 1977. Laboratory Studies of Reinforced Earth using a Woven Polyester Fabric. Proc. Int. Conf. on the Use of Fabric in Geotechnics, Paris, Vol 3, pp 149 - 154.

Holtz, R.D. and Broms, B.B., 1977. Walls Reinforced by Fabrics - Results of Model Tests. Proc Int Conf. on the Use of Fabrics in Geotechnics, Vol 1, pp 113 - 117.

Holtz, R.D., 1985. Soil Reinforcement using Geofabric. Proc 3rd Int. Seminar on Soil Improvement, Singapore, pp 55 - 74.

Ingold, T.S., 1982. Reinforced Earth. Thomas Telford Ltd., London, England.

Jewell, R.A. and Greenwood, J.H., 1988. Long Term Strength and Safety in Steep Slopes Reinforced by Polymer Materials, Dept of Engineering Science, Univ. of Oxford, U.K., Soil Mechanics Report No 083/88, 31 pp.

John, N. W. M., 1986. Geotextile Reinforced Soil Walls in a Tidal Environment. Proc. 3rd Int. Conf. on Geotextiles, Vienna, Vol 2, pp 331 - 336.

John, N.W.M., 1977. Some Considerations on Reinforced Earth Design in the U.K., Proc. Int. Conf. on Soil Reinforcement, Paris, Vol. 1, pp 71 - 76.

John, N., Johnson, P., Ritson, R. and Petley, D., 1982. Behaviour of Fabric Reinforced Soil Walls. Proc 2nd Int. Conf. on Geotextiles, Las Vegas, Vol.3, pp 569 - 574.

Jones, C. J. F. P., 1985. Earth Reinforcement and Soil Structures. Butterworth and Co (Publishers) Ltd., London, England.

Lee, K.L., Adams, B.D. and Vagneron, J.M.J., 1973. Reinforced Earth Retaining Walls. Journ. of the Soil Mech. and Found. Div., ASCE, Vol. 99, No.SM10, pp 745 - 763.

Lindskog, G. and Eriksson, A., 1974. Rapport angående fältförsök med polyestervåv som jordarmering. (Report over Field Tests with Polyester Fabric as Reinforcement in Soil). Report No 50436, Swedish Geotechnical Institute, 32 pp.

Long, N.T., Legeay, G. and Madani, C., 1983. Soil-Reinforcement Friction in a Triaxial Test. Proc 8th European Conf. on Soil Mech. and Found. Engrg., Improvement of Ground, Helsinki, Vol. 1, pp 381 - 384.

McGown, A., Andrawes, K.Z., and Al-Hasani, M.M., 1978. Effect of Inclusion Properties on the Behaviour of Sand. Geotechnique, Vol. 28, No. 3, pp 327 - 346.

McGown, A., Andrawes, K.Z., Wilson-Fahmy, R.F. and Brady, K.C., 1981. A New Method to Determine the Load-Extension Properties of Geotechnical Fabrics. Transport and Road Research Labroatory, Department of the Environment, Department of Transport, Report no. SR 704.

Miyamori, T., Iwai, S. and Maiuchi, K., 1986. Frictional Characteristics of Non-Woven Fabrics. Proc. 3rd Int. Conf. on Geotextiles, Vienna, Austria, Vol. 3, pp 701 - 705.

Murray, R.T., 1980. Fabric Reinforced Earth Walls: Development of Design Equations. Ground Engrg., Vol. 13, No. 7, Oct 1980, pp 29, 31 - 16.

Myles, B., 1982. Assessment of Soil Fabric Friction by Means of Shear. Proc. 2nd Int. Conf. on Geotextiles, Las Vegas, Nevada, Vol 3, pp 787 - 792.

Myles, B. and Carswell, I.G., 1986. Tensile Testing of Geotextiles. Proc. 3rd Int. Conf. on Geotextiles, Vienna, Austria, Vol. 3, pp 713 - 718.

Saxena, S.K. and Budiman, J.S., 1985. Interface Response of Geotextiles. Proc. 11th Int. Conf. on Soil Mech. and Found. Engrg., San Francisco, Vol 3, pp 1801 - 1804.

Tatsuoka, F., Ando, H., Iwasaki, K. and Nakamura, K. 1986. Performances of Clay Test Embankments Reinforced with a Non-woven Geotextile. Proc. 3rd Int. Conf. on Geotextiles, Vol. 2, pp 355 - 360.

Wichter, L., Risseeuw, P. and Gay, G., 1986. Large-scale Test on the Bearing Behaviour of a Woven-Reinforced Earth Wall. Proc. 3rd Int. Conf. on Geotextiles, Vienna, Austria, Vol 2, pp. 301 - 306.

van Zanten, R.V. (Editor), 1986. Geotextiles and Geomembranes in Civil Engineering, Balkema, 658 pp.